NATIONAL AERONAUTICS AND SPACE ADMINISTRATION

Technical Report 32-1159

Determination of Aerodynamic Damping Coefficients From Wind-Tunnel Free-Flight Trajectories of Non-Axisymmetric Bodies

R.H. Prislin

M.B. Wilson

JET PROPULSION LABORATORY

CALIFORNIA INSTITUTE OF TECHNOLOGY

PASADENA, CALIFORNIA

October 15, 1967

Technical Report 32-1159

Determination of Aerodynamic Damping Coefficients From Wind-Tunnel Free-Flight Trajectories of Non-Axisymmetric Bodies

R.H. Prislin

M.B. Wilson

Approved by:

E. A. Laumann, Manager
Aerodynamic Facilities Section

TECHNICAL REPORT 32-1159

Contents

Contents (contd)

Figures

Abstract

General formulas for estimating the aerodynamic damping coefficient $(C_{m_q} + C_{m_{\dot{\alpha}}})$ from planar free-flight oscillation histories are presented. Using Jaffe's energy–integral equation (a phase plane integral of the motion), systematic approximations are introduced that lead to the derivation of accurate results for highly nonlinear and asymmetric static aerodynamics. Particular attention has been given to making the results valid, even for large initial amplitudes and for extreme asymmetries. Two examples are presented to demonstrate the accuracies involved with the various approximations and to illustrate the computational procedure needed for actual data reduction.

Determination of Aerodynamic Damping Coefficients From Wind-Tunnel Free-Flight Trajectories of Non-Axisymmetric Bodies

I. Introduction

A. Preliminary Remarks

Free-flight testing techniques have become increasingly useful in the wind-tunnel study of high-speed aerodynamic characteristics. During the past 4 yr, the Jet Propulsion Laboratory (JPL) has put considerable effort into the development of these techniques for use in conventional wind tunnels. Reference 1 provides a good survey of the work accomplished to date.

The primary value of free-flight testing lies in the absence of model support interference. Furthermore, the technique allows an experiment to be conducted in a dynamic environment similar to actual vehicle flight, rather than in the standard static mode. Therefore, one very important application of such testing techniques is the determination of aerodynamic force and moment coefficients and, in particular, obtaining the aerodynamic damping moment coefficient $(C_{m_q} + C_{m_{\dot{\alpha}}})$, more often

called the dynamic stability derivative. Studies at JPL and elsewhere have generated successful methods of deducing this damping coefficient from the planar oscillatory history provided by free-flight test data, (e.g., Refs. 2, 3, and 4). Thus far, the studies have dealt exclusively with axisymmetric configurations that have their centers-of-gravity on the centerline axis of the bodies. The corresponding symmetry in the vehicle aerodynamics leads to certain simplifications of trajectory analysis and the resulting data reduction. However, this is a restriction that precludes the possibility of analyzing data corresponding to asymmetric configurations, such as lifting bodies, as well as axisymmetric shapes with offset centers of gravity. In anticipation of future interest in the free-flight testing of such configurations, this report discusses some initial studies aimed at the problem of obtaining dynamic stability derivatives from the planar free-flight trajectories of non-axisymmetric vehicles. We make the restriction of planar motion and, in so doing, confine the report to bodies with a plane of symmetry, but not necessarily an axis of symmetry.

B. Some Elementary Equations of Statics

To determine dynamic coefficients from free-flight trajectory data it is necessary to have complete knowledge of the vehicle's static aerodynamics. In general, the static coefficients can be obtained from the free-flight trajectory prior to dynamic analysis (Ref. 2). In this report, it will be assumed that these coefficients are known. Because the static aerodynamics can be given in several forms, it is useful to specify which notations have been used. Consider an arbitrarily shaped body (with a plane of symmetry) at static equilibrium in a uniform flow, V_∞. Because the motion is confined to one plane, say the vertical plane, only two directions are needed to specify the forces acting on the body. Define the axial and normal forces, F_A and F_N, as shown in Fig. 1a. Lift L and drag D are defined in the usual fashion. Resolving these forces, we get the following two sets of equations relating the aerodynamic coefficients C_L, C_D, C_N, and C_A:

$$\left. \begin{array}{l} C_L = C_N \cos \alpha - C_A \sin \alpha \\ C_D = C_N \sin \alpha + C_A \cos \alpha \end{array} \right\} \quad (1)$$

$$\left. \begin{array}{l} C_N = C_L \cos \alpha + C_D \sin \alpha \\ C_A = - C_L \sin \alpha + C_D \cos \alpha \end{array} \right\} \quad (2)$$

The same relations apply for an axisymmetric shape with an offset center of gravity (cg) (Fig. 1b). In either case, the reference axis is taken through the cg so that the dynamic equations remain as simple as possible.

Summation of the moments about the vehicle's cg gives

$$M_{cg} = F_A (e_z) - F_N (l_{cp} - l_{cg}) \quad (3)$$

or in coefficient form

$$C_m = C_A \left(\frac{e_z}{d} \right) - C_N \left(\frac{l_{cp} - l_{cg}}{d} \right) \quad (4)$$

where e_z is the center of pressure (cp) offset normal to the reference axis, d is the reference length, and $l_{cp} - l_{cg}$ is the distance between the cp and cg along the reference axis.

For any particular vehicle configuration, the static coefficients C_L, C_D, and C_m are, themselves, functions of the angle-of-attack, α. As it is not desired to put restrictions on the vehicle oscillation amplitude, it is anticipated that the cp location will also vary with α, i.e., $(l_{cp} - l_{cg})$, as well as e_z, may be functions of α. Nevertheless, the Eqs. (1–4) may always be applied at any fixed α to relate the static coefficients.

Figure 2 shows the general types of static aerodynamics considered in this report. Note that for an axisymmetric body with an offset cg, the offset has no effect on the lift and drag curves. However, the moment curve is altered so that the axisymmetric methods of Refs. 2, 3, and 4 do not apply. No restrictions on the linearity of the coefficients are imposed.

C. Equations of Planar Motion

The coordinate system used for the analysis is shown in Fig. 3, where $x_m - z_m$ is an inertial axis system, fixed with respect to the wind tunnel. It is with reference to this axis system that all measurements of the model's positions are made. However, for analysis purposes, distances must be equivalent to those traveled by a corresponding vehicle moving through still air. The measured value in the z_m direction is correct, but the x_m distance is incorrect because of the wind-tunnel's free-stream velocity. Therefore, the X-Z axis system is defined as fixed with respect to the moving media. Prior to data reduction, the following transformation equations must be applied (Fig. 3):

$$X = x_m + V_\infty t$$

$$\dot{X} = \dot{x}_m + V_\infty$$

$$\ddot{X} = \ddot{x}_m \quad (5)$$

Because of the aerodynamic lift force, a model velocity in the Z-direction is induced; $\dot{z}_m = \dot{Z}$. The actual vehicle velocity V in the X-Z coordinate system is the vector sum of the three velocities V_∞, $\dot{x}_m$, $\dot{z}_m$ and, in general, will not be parallel to the X-axis. The model angle-of-attack, α, defined as the angle between the velocity vector and the model reference axis, cannot be measured directly from wind-tunnel data. Therefore, the equation of angular motion will be written in terms of the more convenient angle θ (Fig. 3). Portions of the ensuing derivation of this equation of angular motion are substantially equivalent to the derivation of Ref. 4. However, the entire development is included here for purposes of clarity and completeness.

$$L = q_\infty A C_L \qquad F_N = q_\infty A C_N$$
$$D = q_\infty A C_D \qquad F_A = q_\infty A C_A$$
$$q_\infty = 1/2\,\rho V_\infty^2$$
$$M = q_\infty A d C_m$$

(b)
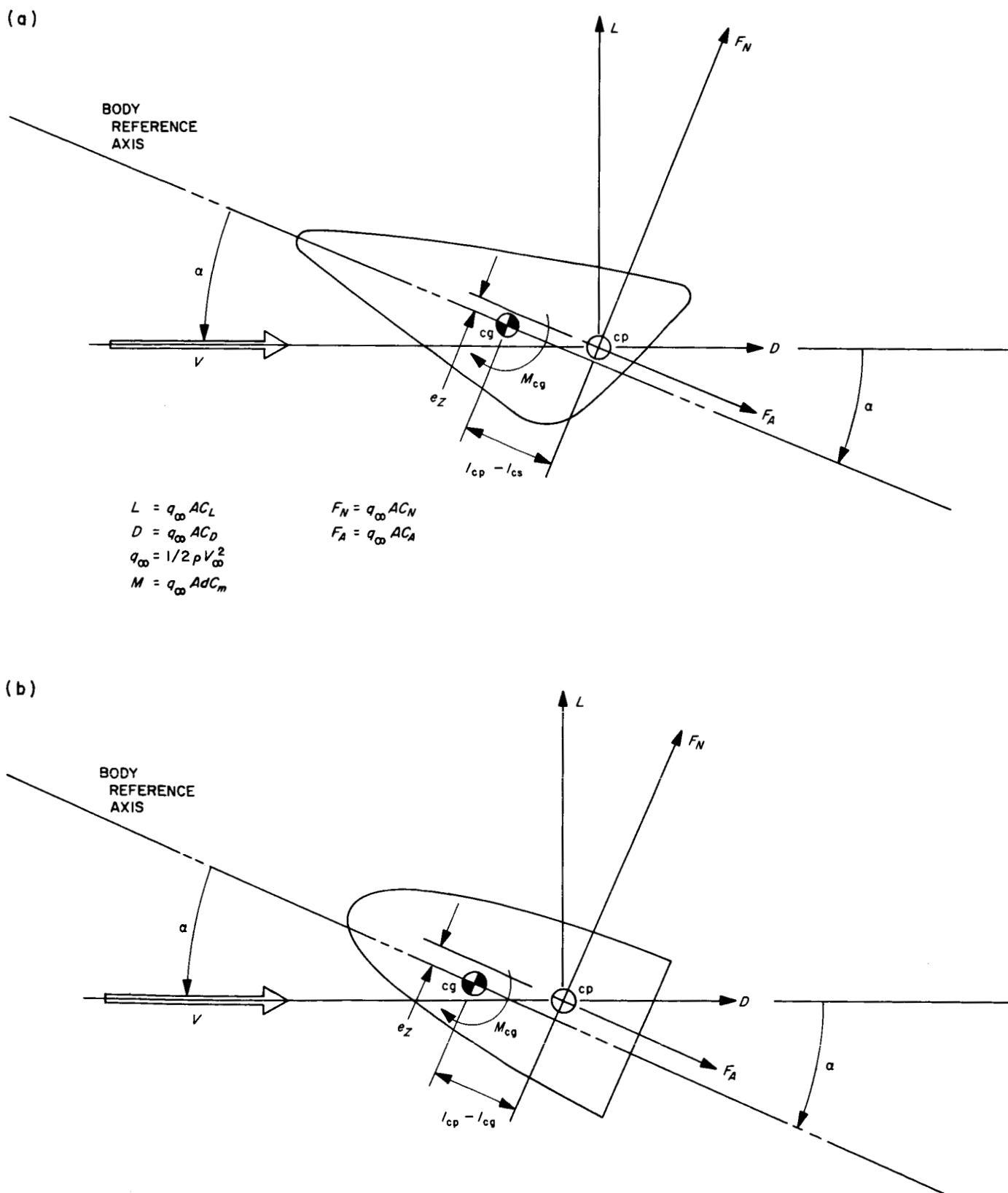
Fig. 1. Definition sketches for force and moment conventions
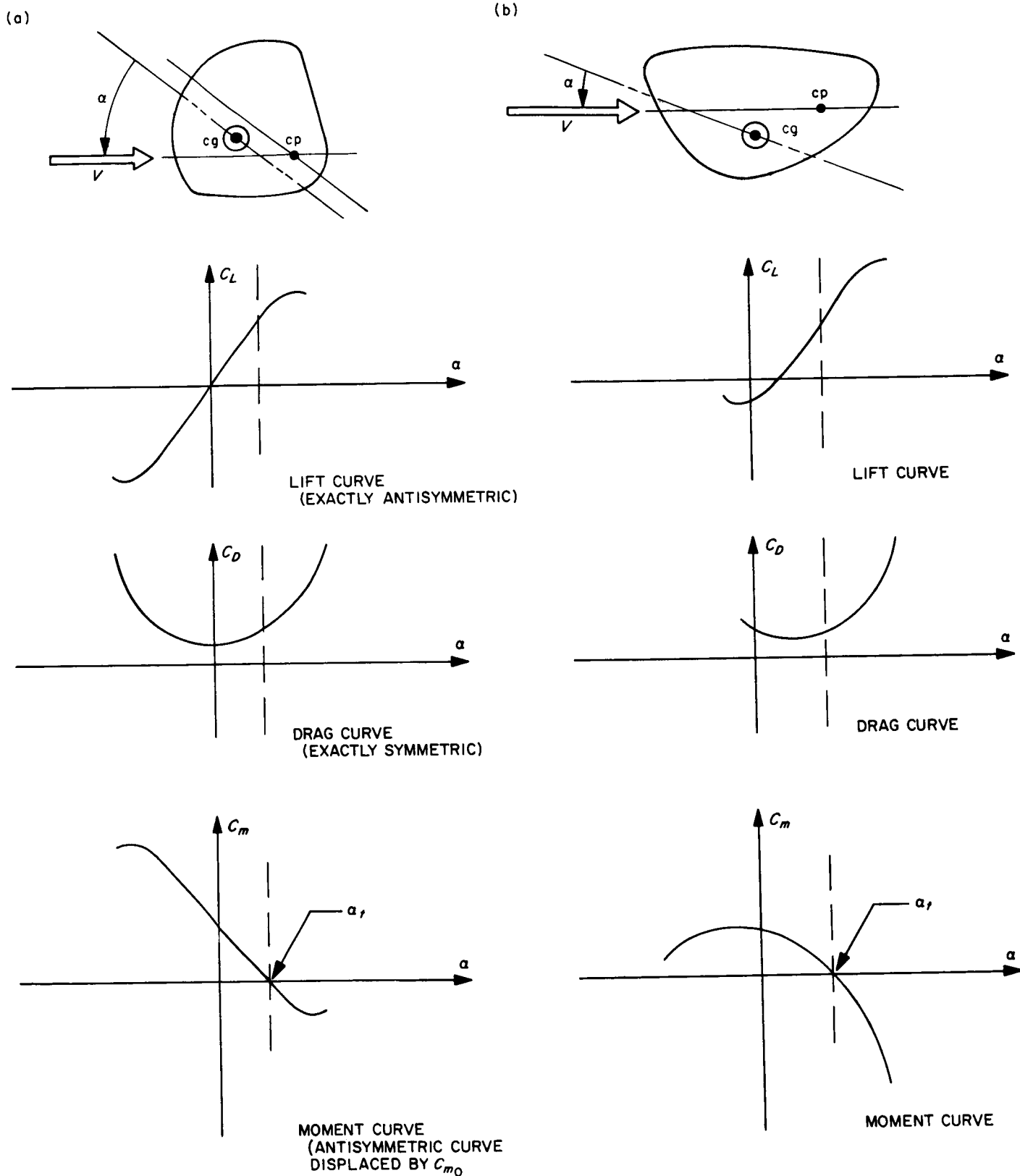
Fig. 2. Schematic representations of body shapes and corresponding static aerodynamics
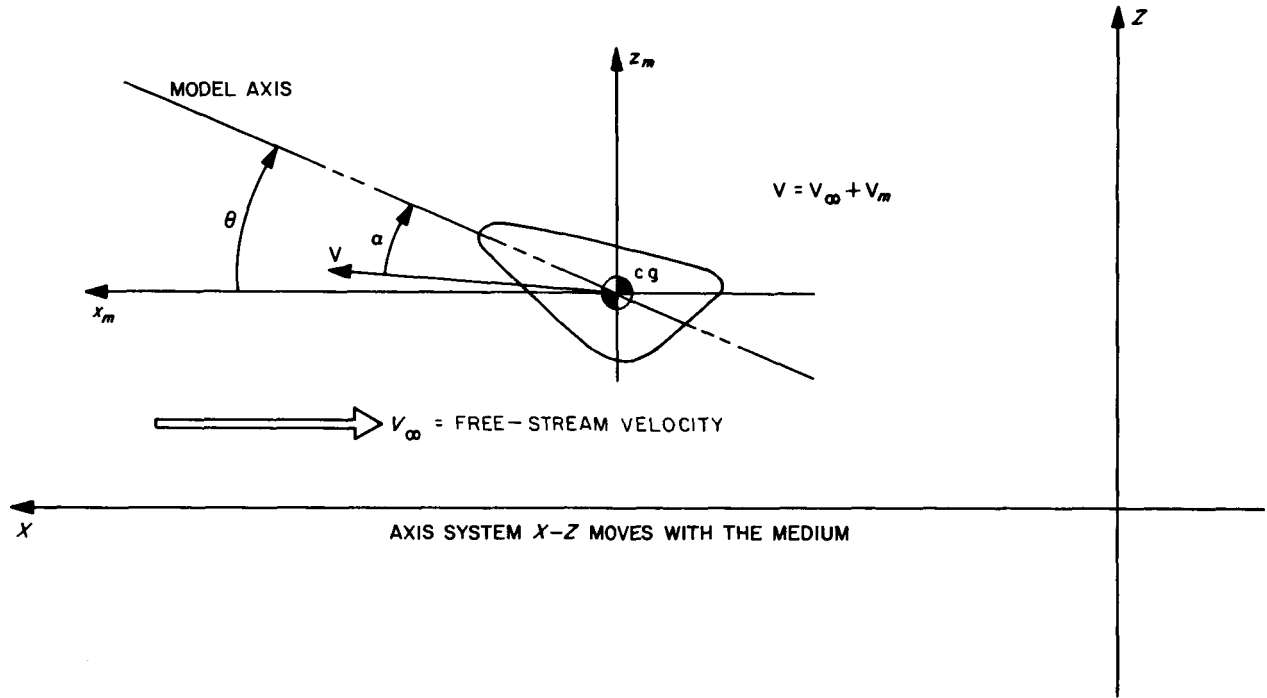
Fig. 3. Data reduction coordinate system

Applications of Newton's second law yield the following equations of planar angular motion and horizontal and vertical translational motions:

$$\sum M_{cg} = I\ddot{\theta} = \frac{1}{2}\rho V^2 A d\left[C_m + C_{m_q}\left(\frac{\dot{\theta}d}{V}\right) + C_{m_{\dot{\alpha}}}\left(\frac{\dot{\alpha}d}{V}\right)\right] \tag{6}$$

$$\sum F_x = m\ddot{X} = -\frac{1}{2}\rho V^2 A C_D \tag{7}$$

$$\sum F_z = m\ddot{Z} = \frac{1}{2}\rho V^2 A C_L - mg \tag{8}$$

Changing the independent variable from time to distance in Eq. (6),

$$\theta''\dot{X}^2 + \theta'\ddot{X} = \frac{\rho A d}{2I}V^2\left[C_m + C_{m_q}\left(\frac{\theta'\dot{X}d}{V}\right) + C_{m_{\dot{\alpha}}}\left(\frac{\alpha'\dot{X}d}{V}\right)\right] \tag{9}$$

For a typical wind-tunnel case, the velocity vector is dominated by the V_∞ term and the angle between V and the X-axis is very small, less than 1 deg. Therefore, a small angle approximation may be employed. Referring to Fig. 3, we note the following:

$$\dot{X} = V\cos(\theta - \alpha) \approx V \tag{10}$$

$$\dot{Z} = V\sin(\theta - \alpha) \approx \dot{X}(\theta - \alpha) \tag{11}$$

Substituting in Eq. (9),

$$\theta'' = \frac{\rho A d}{2I}\left[C_m + (C_{m_q} + C_{m_{\dot{\alpha}}})\,\theta'd - (\theta' - \alpha')\,C_{m_{\dot{\alpha}}}d + \frac{I}{md}C_D\theta'\right] \tag{12}$$

The static pitching moment C_m is a function of α.[1] From expanding the function $C_m(\alpha)$ about θ in a Taylor series and ignoring the higher order powers of $(\theta - \alpha)$,

$$C_m(\alpha) = C_m(\theta) + (\alpha - \theta)\frac{dC_m(\theta)}{d\theta} \tag{13}$$

From differentiating Eq. (11) and using Eq. (7),

$$\ddot{Z} = \ddot{X}(\theta - \alpha) + \dot{X}(\dot{\theta} - \dot{\alpha}) = -\frac{\rho A \dot{X}^2}{2m}C_D(\theta - \alpha) + \dot{X}^2(\theta' - \alpha') \tag{14}$$

Combining Eqs. (8) and (14),

$$\alpha' - \theta' = -\frac{\rho A}{2m}C_L + \frac{g}{\dot{X}^2} + \frac{\rho A}{2m}C_D(\alpha - \theta) \tag{15}$$

The third term on the right side is about two orders of magnitude smaller than the first and it will be ignored. Integrating Eq. (15) with respect to X,

$$(\alpha - \theta) = (\alpha - \theta)_0 + \int_{-\theta_0}^{0}\left(-\frac{\rho A}{2m}C_L + \frac{g}{\dot{X}^2}\right)\frac{d\theta}{\theta'} \tag{16}$$

where $-\theta_0$ is the angle corresponding to $X = 0$.

The lift coefficient C_L, which appears in Eq. (16), and the drag coefficient C_D, which appears in Eq. (12), are also functions of α. However, they comprise second-order effects in the moment equation and, because θ is about equal to α, they can be assumed to be functions of θ directly with a negligible error resulting. Also, normally $|\theta'| >> |\theta' - \alpha'|$ and in general $|C_{m_q}| >> |C_{m_{\dot{\alpha}}}|$; therefore, the third term on the right side of Eq. (12) is negligible. By control of the initial conditions, i.e., $\dot{Z}_0 = 0$, we can have $(\alpha - \theta)_0 = 0$. Finally, for a wind-tunnel free-flight application, gravity terms have no appreciable effect. Incorporating these facts into a combination of Eqs. (12) and (16) yields the following integral–differential equation of angular motion:

$$\theta'' - \frac{\rho A d}{2I}C_m(\theta) + \frac{\rho A d}{2I}\left(\frac{\rho A}{2m}\right)\frac{dC_m(\theta)}{d\theta}\int_{-\theta_0}^{0}\frac{C_L(\theta)}{\theta'}d\theta - \frac{\rho A}{2m}C_D(\theta)\,\theta' - \frac{\rho A d^2}{2I}(C_{m_q} + C_{m_{\dot{\alpha}}})\,\theta' = 0 \tag{17}$$

---

[1] The static aerodynamic coefficients will, in general, also vary with the Mach number. However, because of the extreme dominance of the V_∞ term in the model velocity (supersonically about 98%), the Mach number is assumed to remain constant for the flight.

The problem, then, consists of solving the nonlinear integral–differential, Eq. (17), and inverting the solution to obtain $(C_{m_q} + C_{m_{\dot\alpha}})$ as a function of θ and X. The accuracy of the final expression for the damping derivative depends on the validity of the assumptions made both in the development and solution of Eq. (17). It is, therefore, instructive to summarize the assumptions used to this point and, to mention some common restrictions usually placed on this type of problem but which have not been or will not be imposed in this report.

With the exception of dropping the gravity term, there have been only two assumptions made. The first is that $(\theta - \alpha)$ is a very small angle. The effects of this small angle have been ignored in second-order (and higher) terms, and handled in an approximate manner in the primary term. The second assumption is that the static pitching moment is the main moment acting, and all other terms of the moment equation have second-order effects. For a wind-tunnel application, these two suppositions do not result in any significant errors, even when integrations are performed over long time periods. Therefore, Eq. (17) is nearly an exact expression for planar angular motion.

No mention has been made of the functional dependence of $(C_{m_q} + C_{m_{\dot\alpha}})$. The dynamic stability derivative is usually regarded as an effective constant coefficient over a fixed time period (e.g., the flight time, one-half the flight time, one oscillation cycle, etc.). This is not really a limitation because, by testing at various amplitudes (or frequencies, etc.), an effective coefficient vs amplitude curve can be obtained and, if desired, from this the damping derivative (as a function of instantaneous angular displacement) may be determined (Ref. 5). No restrictions of linearity of static aerodynamics or small angular excursions have been made in the derivation of Eq. (17).

D. Scope of The Report

The primary motivation for the present study was to develop analytical tools capable of handling cases of non-axisymmetric bodies or axisymmetric bodies with a cg offset. The established energy–integral approach used in Refs. 2, 3, and 4 was regarded as one possible method, but not necessarily the only or best approach. Considerable effort was expended into investigating alternate procedures and fresh viewpoints for the solution of the differential Eq. (17). Examples are small perturbation techniques (Ref. 6) and transform methods that simplify the original differential equation (Ref. 7). However, all other approaches investigated led to more serious approximations and more complicated solutions than those re-sulting from the energy–integral approach. Therefore, the work presented in this report consists primarily of applications of the energy integral equations to various sets of nonlinear aerodynamics.

To solve Eq. (17), it is necessary to have explicit functional relationships between the static aerodynamic coefficients and the angle θ. Because any continuous function can be represented as a power series expansion, it is natural to consider many-termed polynomials for C_D, C_L, and C_m. Lift and drag are of second-order influence on the motion and, therefore, such representations offer no particular problems, as approximations may be made in the evaluation of resulting integrals without significant loss of accuracy. However, the same freedom of approximation is not available when considering the primary term: the pitching moment. Consequently, the main limitation on nonlinearities and the corresponding generality of the solution must be imposed on the pitching moment.

Throughout the remainder of this report, lift and drag coefficients will be considered with the following functional representations:

$$\left.\begin{array}{l} C_L(\theta) = C_{L_0} + C_{L_\alpha}\theta + C_{L_1}\theta^2 + C_{L_2}\theta^3 \\[2mm] C_D(\theta) = C_{D_0} + C_{D_1}\theta + C_{D_2}\theta^2 + C_{D_3}\theta^3 + C_{D_4}\theta^4 \end{array}\right\} \quad (18)$$

Additional terms for these series expansions could be handled without too great of an increase in complexity. However, these particular curves are sufficiently general to be representative of a large class of shapes, and more terms would not be necessary. The following four alternate pitching moment curves are considered in detail:

(1) Case 1, offset linear moment:

$$C_m(\theta) = C_{m_0} + C_{m_\alpha}\theta \quad (19)$$

(2) Case 2, bi-linear moment:

$$\left.\begin{array}{ll} C_m(\theta) = C_{m_{\alpha-}}\theta, & \theta \le 0 \\[2mm] C_m(\theta) = C_{m_{\alpha+}}\theta, & \theta \ge 0 \end{array}\right\} \quad (20)$$

(3) Case 3, bi-cubic moment:

$$\left.\begin{array}{ll} C_m(\theta) = C_{m_\alpha}\theta + 2C_{m_{2-}}\theta^3, & \theta \le 0 \\[2mm] C_m(\theta) = C_{m_\alpha}\theta + 2C_{m_{2+}}\theta^3, & \theta \ge 0 \end{array}\right\} \quad (21)$$

(4) Case 4, full cubic moment:

$$C_m(\theta) = C_{m_\alpha}\theta + 3/2\,C_{m_1}\theta^2 + 2C_{m_2}\theta^3 \qquad (22)$$

For cases 2, 3, and 4 it is required that $C_m(0) = 0$. This actually does not constitute a restriction because the model reference axis can always be defined so that $\theta = 0$ at the model trim position.

The first phase of the analysis consists of the derivation of closed-form solutions for the dynamic stability derivatives of a vehicle exhibiting static aerodynamics as given by Eqs. (18–22). The first three pitching moment forms listed are completely analyzed. For the full-cubic moment, several case distinctions would be necessary for a complete analysis; only the physically most likely of these cases is considered. Nevertheless, the solution is much more complex than those corresponding to the other pitching moments. This particular case, therefore, illustrates that for longer or more complicated functional forms of pitching moments an analytical approach is not practical, and numerical techniques should be employed.

The limitation of closed-form solutions corresponding only to the pitching moments, given by Eqs. (19–22), imposes a serious restriction on the applicability of these solutions. However, the motion of a body exhibiting an arbitrary pitching moment can be analyzed by assuming one of the simpler moment shapes. The criteria and methodology for determining an approximating curve, given the original pitching moment and the free-flight trajectory, is the subject of the second phase of this analysis.

As a verification of the validity and accuracy of the results presented here, the equations have been applied to two sample cases. A six-degree-of-freedom computer program was used to calculate trajectories corresponding to the two cases of nonlinear static aerodynamics. The equations derived in this report were used to calculate dynamic stability derivatives from the trajectory outputs of the program. Comparison of the calculated value of $(C_{m_q} + C_{m_{\dot\alpha}})$ with the input value allows a direct verification of the accuracy of the formulas derived.

II. The Energy Integral Relation and Its Application

A. An Integral of Planar Motion

The coefficients of the differential Eq. (17) are functions of θ and θ', and do not explicitly contain X. This suggests considering the motion in the phase plane (θ' vs θ plane) rather than the coordinate plane (Fig. 4). This
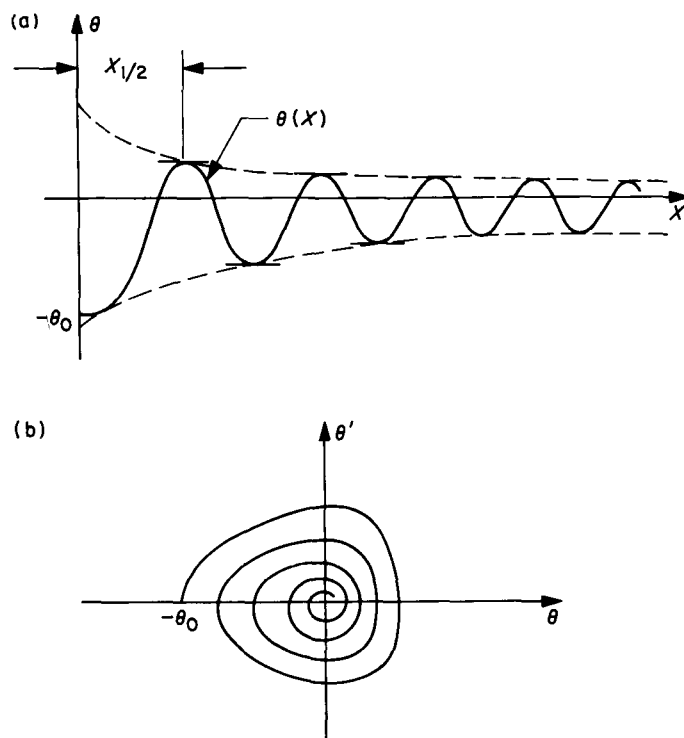
Fig. 4. Comparison of motion in coordinate and phase planes

means eliminating dX in the differential equation in favor of terms involving $d\theta'$. Using the relations $\theta'' = d\theta'/dX$ and $\theta' = d\theta/dX$ and multiplying the differential equation through by $\theta'\,dX$,

$$\theta'd\theta' = \frac{\rho A d}{2I}C_m(\theta)\,d\theta - \frac{\rho A d}{2I}\left(\frac{\rho A}{2m}\right)\frac{dC_m(\theta)}{d\theta}$$
$$\times\left[\int_{-\theta_0}^{\theta}\frac{C_L(\theta)}{\theta'}d\theta\right]d\theta$$
$$+ \frac{\rho A}{2m}C_D(\theta)\,\theta'd\theta + \frac{\rho A d^2}{2I}(C_{m_q} + C_{m_{\dot\alpha}})\,\theta'd\theta$$

$$(23)$$

For notational convenience, assume (without loss of generality) the body has an initial angle $-\theta_0 < 0$. Define θ_1 as the positive angle to which the vehicle would oscillate in ½ cycle if the system were completely conservative; i.e., if the static pitching moment were the only moment acting. Therefore, θ_1 is the angle that results in a net change of zero in potential energy resulting from $C_m(\theta)$ over ½ cycle,

$$\int_{-\theta_0}^{\theta_1} C_m(\theta)\,d\theta = 0 \qquad (24)$$

Equation (24) provides a method of calculating θ_1, given the angle $-\theta_0$ and the pitching moment curve. Define $\delta\theta$ as the loss in amplitude over ½ cycle as a result of the dissipated energy from the combined damping effects. In general, $\theta_1 \gg \delta\theta$ and, therefore, when integrating Eq. (25) over ½ cycle, the upper limit of integration $(\theta_1 - \delta\theta)$ may be replaced by θ_1 in all the second-order terms.[2] Also at the two amplitude peaks, $-\theta_0$ and $(\theta_1 - \delta\theta)$ the angular velocity $\theta' = 0$. Therefore, integrating Eq. (23) over ½ an oscillation cycle and solving algebraically for the dynamic stability coefficient,

$$(C_{m_q} + C_{m_{\dot\alpha}})\frac{md^2}{I} = \frac{\dfrac{-md}{I}\displaystyle\int_{-\theta_0}^{\theta_1-\delta\theta} C_m(\theta)\,d\theta + \dfrac{\rho Ad}{2I}\displaystyle\int_{-\theta_0}^{\theta_1}\left[\dfrac{dC_m(\theta)}{d\theta}\displaystyle\int_{-\theta_0}^{\theta}\dfrac{C_L(\theta)}{\theta'}\,d\theta\right]d\theta - \displaystyle\int_{-\theta_0}^{\theta_1} C_D(\theta)\,\theta'\,d\theta}{\displaystyle\int_{-\theta_0}^{\theta_1}\theta'\,d\theta}$$

(25)

The equation for the damping coefficient in this form was first derived by Jaffe (Ref. 3) and has been called the energy-integral relation.

To perform all the integrations indicated by Eq. (25) it is necessary to have an explicit expression for θ' in terms of θ. This can be obtained by ignoring all terms on the right side of Eq. (23) except the predominant pitching moment, as follows:

$$\theta'\,d\theta' = \frac{\rho Ad}{2I} C_m(\theta)\,d\theta$$

(26)

$$\theta' = (2k_m)^{1/2}\left[\int_{-\theta_0}^{\theta} C_m(\theta)\,d\theta\right]^{1/2}$$

(27)

where $k_m = \rho Ad/2I$. This estimate is an adequate representation in most physical cases. An iterative procedure to improve on it can be set up by using Eq. (27) as a first estimate, and repeatedly applying Eq. (23) to obtain progressively better approximations. However, the integrals become cumbersome very rapidly and, in general, the increase in accuracy is insignificant and unnecessary.

It will be convenient to state the energy integral equation in a standard form for reference purposes. Consider the first integral in the numerator of Eq. (25), as follows:

$$-\frac{md}{I}\int_{-\theta_0}^{(\theta_1-\delta\theta)} C_m(\theta)\,d\theta = -\frac{md}{I}\left[\int_{-\theta_0}^{\theta_1} Cm(\theta)\,d\theta + \int_{\theta_1}^{\theta_1-\delta\theta} Cm(\theta)\,d\theta\right]$$

(28)

The first term on the right vanishes by definition of θ_1. The second integral can be evaluated approximately (to excellent accuracy) by using the trapezoid rule and the fact that $\theta_1 \gg \delta\theta$,

$$-\frac{md}{I}\int_{\theta_1}^{\theta_1-\delta\theta} C_m(\theta)\,d\theta \approx -\frac{md}{I}(-\delta\theta)\frac{C_m(\theta_1) + C_m(\theta_1 - \delta\theta)}{2} \approx \frac{md}{I}\delta\theta C_m(\theta_1)$$

(29)

Equation (25) can be represented as follows:

$$(C_{m_q} + C_{m_{\dot\alpha}})\frac{md^2}{I} = \frac{\dfrac{md}{I}\delta\theta C_m(\theta_1)}{\displaystyle\int_{-\theta_0}^{\theta_1}\theta'\,d\theta} + \text{lift term} - \text{drag term}$$

(30)

---

[2]This is an approximation that does not need to be made when discussing numerical integrations later in the report. However, it makes no significant difference and, therefore, the point is not mentioned at that time.

For a wind-tunnel application, the first term on the right side usually comprises from 70 to 95% of the total. Therefore, the evaluation of the integral in the denominator of that term becomes the most important calculation when considering the accuracy of the final answer.

There is one additional equation that will be useful in succeeding sections. This is an estimate for the ½-cycle distance period of oscillation. By using $\theta' = d\theta/dX$,

$$X_{\frac{1}{2}} = \int_{-\theta_0}^{\theta_1} \frac{d\theta}{\theta'} = \int_0^{\theta_1} \frac{d\theta}{\theta'} - \int_0^{-\theta_0} \frac{d\theta}{\theta'} \tag{31}$$

Equation (27) may be used to substitute for θ' and the result integrated to obtain $X_{\frac{1}{2}}$. This equation will be used in a later section to aid in the calculation of coefficients for an approximating moment curve from an experimentally measured distance period.

In a sense, Eqs. (25) and (27) comprise a complete solution to the general planar motion problem. Given the static aerodynamics in either functional or tabulated form and the angles $-\theta_0$ and $(\theta_1 - \delta\theta)$ from an experimental oscillatory history, these equations may always be integrated numerically to obtain a value for $(C_{m_q} + C_{m_{\dot{\alpha}}})$. However, it is still advantageous to solve the equations analytically for the most general case possible. A closed-form solution (in addition to its ease of application) can be far more useful in parametric studies than a numerical integration and affords the investigator an immediate method to explore the relative importance of various terms in the differential equation of motion. The basic equations necessary for a complete analytical solution are Eqs. (24), (25), (27), and (31). The application of these equations collectively will be referred to as the energy–integral method. The next four sections of this report use the energy–integral method to obtain solutions for the dynamic derivative corresponding to four particular pitching moment curves.

B. Offset Linear Pitching Moment: $C_m(\theta) = C_{m_0} + C_{m_\alpha}\theta$

1. Calculation of θ_1 from conservation of energy.

$$\int_{-\theta_0}^{\theta_1} C_m(\theta)\, d\theta = 0 = C_{m_0}\theta_1 + \frac{C_{m_\alpha}}{2}\theta^2 + C_{m_0}\theta_0 - \frac{C_{m_\alpha}}{2}\theta_0^2 \tag{32}$$

By solving this quadratic for θ_1,

$$\theta_1 = \theta_0 - 2r$$

where

$$r = C_{m_0}/C_{m_\alpha} \tag{33}$$

2. Estimate of θ'.

$$\theta' = (2k_m)^{\frac{1}{2}} \left[\int_{-\theta_0}^{\theta} (C_{m_0} + C_{m_\alpha}\theta)\, d\theta \right]^{\frac{1}{2}} = (2k_m)^{\frac{1}{2}} \left[\frac{C_{m_\alpha}}{2}\theta^2 + C_{m_0}\theta + \left(C_{m_0}\theta_0 - \frac{C_{m_\alpha}}{2}\theta_0^2 \right) \right]^{\frac{1}{2}} \tag{34}$$

3. Estimate of ½-cycle distance period, $X_{\frac{1}{2}}$.

$$X_{\frac{1}{2}} = \frac{1}{(2k_m)^{\frac{1}{2}}} \int_{\theta_0}^{\theta_1} \frac{d\theta}{\left[\frac{C_{m_\alpha}}{2}\theta^2 + C_{m_0}\theta + \left(C_{m_0}\theta_0 - \frac{C_{m_\alpha}}{2}\theta_0^2 \right) \right]^{\frac{1}{2}}} = \frac{1}{(-k_m C_{m_\alpha})^{\frac{1}{2}}} \left[\sin^{-1}\left(-\frac{(C_{m_\alpha}\theta_1 + C_{m_0})}{C_{m_0} - C_{m_\alpha}\theta_0} \right) + \frac{\pi}{2} \right] \tag{35}$$

By substituting Eq. (33) for θ_1

$$X_{\frac{1}{2}} = \frac{\pi}{(-k_m C_{m_\alpha})^{\frac{1}{2}}} \tag{36}$$

4. Aerodynamic damping coefficient. Using the lift and drag curves of Eq. (18) and the offset linear pitching moment and corresponding angular velocity in the energy–integral equation, the following solution results:

$$(C_{m_q} + C_{m_{\dot\alpha}})\frac{md^2}{I} = -\frac{2\delta\theta}{\pi(\theta_0 - r)}\frac{md}{I}\left(-\frac{C_{m_\alpha}}{k_m}\right)^{1/2} + \text{lift term} - \text{drag term} \tag{37}$$

$$\text{Lift term} = -\frac{2C_{L_0}}{(\theta_0 - r)} + C_{L_\alpha}\left(1 + \frac{2r}{\theta_0 - r}\right) - C_{L_1}\left(2r - 3r^2 + \frac{\theta_0(\theta_0 - 2r)}{\theta_0 - r}\right)$$
$$+ C_{L_2}\left[\frac{11}{3}r^2 + \frac{1}{12}(\theta_0 - r)^2 + \frac{2}{3}\theta_0(\theta_0 - 2r) + \frac{r(5r^2 - 6r\theta + 3\theta)}{\theta_0 - r}\right] \tag{38}$$

$$\text{Drag term} = C_{D_0} - C_{D_1}r + C_{D_2}\left[r^2 + \frac{1}{4}(\theta_0 - r)^2\right] - C_{D_3}\left[\frac{7}{4}r^3 - \frac{3}{2}\theta_0 r\left(1 - \frac{1}{2}\theta_0\right)\right]$$
$$+ C_{D_4}\left[\frac{21}{5}r^2\left(r + \frac{1}{4}(\theta_0 - r)^2\right) - \frac{841}{180}r^2\theta_0\left(r - \frac{1}{2}\theta_0\right) + \theta_0^2\left(r - \frac{1}{2}\theta_0\right)^2\right] \tag{39}$$

The first term on the right-hand side of Eq. (37) can be put into a simpler form by using Eq. (36) as follows:

$$-\frac{2\delta\theta}{\pi(\theta_0 - r)}\frac{md}{I}\left(-\frac{C_{m_\alpha}}{k_m}\right)^{1/2} = -\frac{4m}{\rho A}\frac{1}{X_{1/2}}\frac{\delta\theta}{(\theta_0 - r)} \tag{40}$$

5. Solution for axisymmetric shapes. For an axisymmetric body with its cg on the vehicle centerline, the drag curve would be symmetric about the line $\theta = 0$, and would, therefore, have an even-power series representation. The lift and pitching moment curves would be antisymmetric and have odd-power series expansions. Therefore, for an axisymmetric body with a linear pitching moment, Eqs. (37), (38), and (39) apply when C_{m_0}, C_{L_0}, C_{L_1}, C_{D_1}, and C_{D_3} are set equal to zero. The resulting formula is then identical to equations presented in Ref. 2.

C. Bi-Linear Pitching Moment

The most obvious, and perhaps the most useful, technique for dealing with a nonsymmetric moment curve is to approximate the plus and minus portions of the actual moment by two straight lines through the origin, as follows:

$$\left.\begin{aligned} C_m(\theta) &= C_{m_{\alpha-}}\theta, & \theta &\leq 0 \\ C_m(\theta) &= C_{m_{\alpha+}}\theta, & \theta &\geq 0 \end{aligned}\right\} \tag{41}$$

Because in general, the slopes of the two curves will not be the same, this functional representation has a singularity at $\theta = 0$. Therefore, all integral calculations must be performed separately in the two regions.

1. Calculation of θ_1.

$$\int_{-\theta_0}^{\theta_1} C_m(\theta)\, d\theta = 0 = \int_{-\theta_0}^{0} C_{m_{\alpha-}}\theta\, d\theta + \int_{0}^{\theta_1} C_{m_{\alpha+}}\theta\, d\theta = -C_{m_{\alpha-}}\frac{\theta_0^2}{2} + C_{m_{\alpha+}}\frac{\theta_1^2}{2} \tag{42}$$

By defining $\mu^2 = \theta_1^2/\theta_0^2 = C_{m_{\alpha-}}/C_{m_{\alpha+}}$ the result is as follows:

$$\theta_1 = \mu\theta_0 = \left(\frac{C_{m_{\alpha-}}}{C_{m_{\alpha+}}}\theta_0\right)^{1/2} \tag{43}$$

2. *Estimate of* θ'. Direct substitution in Eq. (27) yields the following two expressions:

$$\left.\begin{array}{l} \theta' = (-k_m C_{m_{\alpha-}})^{1/2}(\theta_0^2 - \theta^2)^{1/2}, \qquad \theta \leq 0 \\[2ex] \theta' = (-k_m C_{m_{\alpha+}})^{1/2}(\theta_1^2 - \theta^2)^{1/2} = (-k_m C_{m_{\alpha-}})^{1/2}\left(\theta_0^2 - \frac{1}{\mu^2}\theta^2\right)^{1/2}, \qquad \theta \geq 0 \end{array}\right\} \tag{44}$$

3. *Estimate of the* ½-*cycle-distance period,* $X_{1/2}$.

$$\begin{aligned} X_{1/2} &= \frac{1}{(-k_m C_{m_{\alpha-}})^{1/2}}\int_{-\theta_0}^{0}\frac{d\theta}{(\theta_0^2 - \theta^2)^{1/2}} + \frac{1}{(-k_m C_{m_{\alpha+}})^{1/2}}\int_{0}^{\theta_1}\frac{d\theta}{(\theta_1^2 - \theta^2)^{1/2}} \\ &= \frac{1}{(-k_m C_{m_{\alpha-}})^{1/2}}\frac{\pi}{2} + \frac{1}{(-k_m C_{m_{\alpha+}})^{1/2}}\frac{\pi}{2} = \frac{\pi/2}{(-k_m C_{m_{\alpha-}})^{1/2}}(1+\mu) \end{aligned} \tag{45}$$

4. *Aerodynamic damping coefficient.* Evaluating the integrals of Eq. (25) in two pieces corresponding to $\theta \leq 0$ and $\theta \geq 0$ and simplifying algebraically results in the following:

$$(C_{m_q} + C_{m_{\dot\alpha}})\frac{md^2}{I} = -\frac{4m}{\rho A}\frac{1}{\mu X_{1/2}}\frac{\delta\theta}{\theta_0} + \text{lift term} - \text{drag term} \tag{46}$$

$$\begin{aligned} \text{Lift term} = &-\frac{2C_{L_0}}{\mu\theta_0} + C_{L_\alpha}\left[1 + \frac{4}{\pi}\frac{(1-\mu)}{\mu}\right] - C_{L_1}\theta_0\left[\frac{1-\mu+\mu^2}{\mu} + \frac{8}{3\pi}(1-\mu)\right] \\ &+ C_{L_2}\theta_0^2\left[\frac{3}{4}(1-\mu+\mu^2) + \frac{8}{3\pi}\frac{(1-\mu)(1+\mu^2)}{\mu}\right] \end{aligned} \tag{47}$$

$$\text{Drag term} = C_{D_0} + C_{D_1}\theta_0\frac{4}{3\pi}(\mu-1) + C_{D_2}\theta_0^2\frac{(1-\mu+\mu^2)}{4} + C_{D_3}\theta_0^3\frac{8}{15\pi}\left(\frac{\mu-1}{\mu+1}\right) + \frac{C_{D_4}\theta_0^4}{8} \tag{48}$$

D. Bi-Cubic Pitching Moment

A natural extension to the idea of the bi-linear moment is to consider two approximating curves, each of which allows nonlinearities in its region of applicability. By using two distinct curves, rather than one higher order polynomial, a greater choice in the functional form is available. Choosing the two approximating curves as odd-power series expansions results in a simplification of subsequent integrals. Therefore, this section deals with the following moment curve:

$$\left.\begin{array}{l} C_m(\theta) = C_{m_\alpha}\theta + 2C_{m_{2-}}\theta^3, \qquad \theta \leq 0 \\[2ex] C_m(\theta) = C_{m_\alpha}\theta + 2C_{m_{2+}}\theta^3, \qquad \theta \geq 0 \end{array}\right\} \tag{49}$$

1. Calculation of θ_1.

$$\int_{-\theta_0}^{\theta_1} C_m(\theta)\,d\theta = 0 = \int_{-\theta_0}^{0} (C_{m_\alpha}\theta + 2C_{m_{2-}}\theta^3)\,d\theta + \int_0^{\theta_1} (C_{m_\alpha}\theta + 2C_{m_{2+}}\theta^3)\,d\theta \tag{50}$$

$$C_{m_{2+}}\theta_1^4 + C_{m_\alpha}\theta_1^2 - C_{m_\alpha}\theta_0^2 - C_{m_{2-}}\theta_0^4 = 0 \tag{51}$$

or

$$\theta_1 = \left\{ \frac{-C_{m_\alpha} \pm [C_{m_\alpha}^2 + 4C_{m_{2+}}(C_{m_\alpha}\theta_0^2 + C_{m_{2-}}\theta_0^4)]^{1/2}}{2C_{m_{2+}}} \right\}^{1/2} \tag{52}$$

The $\pm$ sign under the radical causes no ambiguity because the root desired is the smallest real positive root to Eq. (25).

2. Estimate of θ'.

As in the previous case, the integral calculations must be broken into two parts corresponding to the two segments of the moment curve. For $\theta \leq 0$,

$$\theta' = (2k_m)^{1/2} \left[\int_{-\theta_0}^{0} (C_{m_\alpha}\theta + C_{m_{2-}}\theta^3)\,d\theta \right]^{1/2} = (k_m C_{m_{2-}})^{1/2} (\theta^2 - \theta_0^2)^{1/2} \left(\theta^2 + \frac{C_{m_\alpha}}{C_{m_{2-}}} + \theta_0^2 \right)^{1/2} \tag{53}$$

For $\theta \geq 0$,

$$\theta' = (2k_m)^{1/2} \left[-C_{m_\alpha}\frac{\theta_0^2}{2} - C_{m_{2-}}\frac{\theta_0^4}{2} + \int_0^{\theta} (C_{m_\alpha}\theta + 2C_{m_{2+}}\theta^3)\,d\theta \right]^{1/2} = (k_m)^{1/2} [\,-C_{m_\alpha}(\theta_0^2 - \theta^2) + C_{m_{2+}}\theta^4 - C_{m_{2-}}\theta_0^4]^{1/2} \tag{54}$$

By using Eq. (51) to simplify the latter equation,

$$\theta' = (k_m C_{m_{2+}})^{1/2} (\theta^2 - \theta_1^2)^{1/2} \left(\theta^2 + \frac{C_{m_\alpha}}{C_{m_{2+}}} + \theta_1^2 \right)^{1/2} \tag{55}$$

Equations (53) and (55) show that the angular velocity equation for the second ¼ cycle has the same functional form as the one for the first ¼ cycle; they differ only by the replacement of θ_0 by θ_1 and $C_{m_{2-}}$ by $C_{m_{2+}}$. This is as would be expected from the functional symmetry of the moment curve. Put another way, because the equation being used describes a conservative system, the kinetic energy at any given angle between $-\theta_0$ and θ_1 must be the same, regardless of whether the initial angle was $-\theta_0$ or θ_1. Therefore, the angular velocity at the given angle is also independent (except for sign) of which amplitude peak we start at. It follows from the symmetry in form of the two parts of the moment representation that the results from the first ¼ cycle will also apply to the second ¼ cycle of motion on substitution for the pertinent constants. A similar argument holds for the other integrals involved in the calculations of the distance period and the damping coefficient. Therefore, for this moment, it is sufficient to consider only the first ¼ cycle of motion, and to use these results with a substitution for the values of the integrals over the second ¼ cycle.

3. Estimate of the ½-cycle distance period, $X_{1/2}$.

Consider the first ¼-oscillation cycle, i.e., as θ goes from $-\theta_0$ to 0,

$$X_{1/4} = \int_{-\theta_0}^{0} \frac{d\theta}{\theta'} = -(k_m C_{m_{2-}})^{1/2} \int_0^{-\theta_0} \frac{d\theta}{(\theta^2 - \theta_0^2)^{1/2} \left(\theta^2 + \frac{C_{m_\alpha}}{C_{m_{2-}}} + \theta_0^2 \right)^{1/2}} \tag{56}$$

This integral cannot be evaluated in terms of elementary functions. However, through use of a suitable substitution the integral may be transformed into the Legendre canonical form of an elliptic integral of the first kind (Ref. 8). A

case distinction and alternate substitutions must be made for the two possible algebraic signs of $C_{m_{2-}}$, as follows:

Case 1. Let $C_{m_{2-}} > 0$. The body is statically stable at $-\theta_0$, i.e., $-C_{m_\alpha}\theta_0 - 2C_{m_{2-}}\theta_0^3 > 0$. This implies the following three inequalities:

$$\frac{C_{m_\alpha}}{2C_{m_{2-}}} + \theta_0^2 < 0, \qquad \frac{C_{m_\alpha}}{C_{m_{2-}}} + \theta_0^2 < 0, \qquad -\frac{C_{m_\alpha}}{C_{m_{2-}}} > 2\theta_0^2$$

Let

$k^2 = \theta_0^2 / -(C_{m_\alpha}/C_{m_{2-}} + \theta_0^2) < 1$, and $\phi = \sin^{-1}\theta/\theta_0$ to get the following:

$$X_{1_4} = \left[-\frac{1}{k_m(C_{m_\alpha} + C_{m_{2-}}\theta_0^2)} \right]^{1/2} F\left(k, \frac{\pi}{2}\right) \tag{57}$$

where $F(k, \phi)$ is the Legendre canonical form or normal elliptic integral of the first kind with modulus k and argument ϕ.

Case 2. Let $C_{m_{2-}} < 0$, $k^2 = \theta_0^2/(C_{m_\alpha}/C_{m_{2-}} + 2\theta_0^2)$, $\phi = \cos^{-1}\theta/\theta_0$

The result is as follows:

$$X_{1_4} = \left[-\frac{1}{k_m(C_{m_\alpha} + 2C_{m_{2-}}\theta_0^2)} \right]^{1/2} F\left(k_-, \frac{\pi}{2}\right) \tag{58}$$

Similar results can be obtained for the second $\frac{1}{4}$ cycle with $C_{m_{2+}}$ and θ_1 substituted for $C_{m_{2-}}$ and θ_0, respectively. The $\frac{1}{2}$-cycle distance period is clearly the sum of the applicable $\frac{1}{4}$-cycle results, $X_{1_2} = X_{1_4} + X_{1_4+}$. Thus, there are four possible expressions for the distance period, depending on the four possible sign combinations of the terms $C_{m_{2-}}$ and $C_{m_{2+}}$. The results are summarized in Table 1. The necessary values of the elliptic integral $F(k, \pi/2)$ are readily available in

Table 1. Summary of distance periods over the ¼ cycles

First ¼ cycle		
Sign combinations	k_-^2	X_{1_4-}
$C_{m_{2-}} > 0$	$-\dfrac{\theta_0^2}{\dfrac{C_{m_\alpha}}{C_{m_{2-}}} + \theta_0^2}$	$\dfrac{1}{(k_m)^{1/2}}\left(-\dfrac{1}{C_{m_\alpha} + C_{m_{2-}}\theta_0^2}\right)^{1/2} F\left(k_-, \dfrac{\pi}{2}\right)$
$C_{m_{2-}} < 0$	$\dfrac{\theta_0^2}{\dfrac{C_{m_\alpha}}{C_{m_{2-}}} + 2\theta_0^2}$	$\dfrac{1}{(k_m)^{1/2}}\left(-\dfrac{1}{C_{m_\alpha} + 2C_{m_{2-}}\theta_0^2}\right)^{1/2} F\left(k_-, \dfrac{\pi}{2}\right)$
Second ¼ cycle		
Sign combinations	k_+^2	X_{1_4+}
$C_{m_{2+}} > 0$	$-\dfrac{\theta_1^2}{\dfrac{C_{m_\alpha}}{C_{m_{2+}}} + \theta_1^2}$	$\dfrac{1}{(k_m)^{1/2}}\left(-\dfrac{1}{C_{m_\alpha} + C_{m_{2+}}\theta_1^2}\right)^{1/2} F\left(k_+, \dfrac{\pi}{2}\right)$
$C_{m_{2+}} < 0$	$-\dfrac{\theta_1^2}{\dfrac{C_{m_\alpha}}{C_{m_{2+}}} + 2\theta_1^2}$	$\dfrac{1}{(k_m)^{1/2}}\left(-\dfrac{1}{C_{m_\alpha} + 2C_{m_{2+}}\theta_1^2}\right)^{1/2} F\left(k_+, \dfrac{\pi}{2}\right)$

tabulated form. For reference purposes, Fig. 5 shows this function plotted vs the square of the elliptic modulus, k^2.

4. Aerodynamic damping coefficient. Substitution of the bi-cubic moment and corresponding angular velocity in Eq. (25) again results in integrals that are nonelementary in nature. The most difficult integrations to perform are those which have the least influence on the accuracy of the solution, i.e., the integrals involved in the lift and drag terms. Furthermore, expressions for these two terms that are computed with the integrals assuming the bi-cubic moment are very cumbersome and difficult to apply. Therefore, because the loss in accuracy is small, the lift and drag terms will be handled in an approximate fashion. A succeeding section of this report derives methods of determining the coefficients of any particular (functional form) moment curve that will approximate an arbitrary moment curve. Therefore, given a bi-cubic moment, an approximating bi-linear moment may be determined and used to calculate the effects of lift and drag. Inspection of Eqs. (47) and (48) shows that the quantity

$$\mu = (C_{m_{\alpha-}}/C_{m_{\alpha+}})^{1/2} = \theta_1/\theta_0$$

describes the dependence on the pitching moment of the lift and drag terms. Because θ_0 and θ_1 are known, they may be used directly to calculate μ, and the approximating moment curve need not be actually displayed. (The physical meaning and justification of this step will become clear in the following section.) Equations (47) and (48) will be used to approximate the lift and drag terms.

The problem is, therefore, reduced to the evaluation of the denominator of Eq. (25), the integral,

$$\int_{-\theta_0}^{\rho_1} \theta' d\theta$$

It is interesting, at this point, to investigate the magnitude of the error that would be introduced were a bi-linear moment used to approximate a bi-cubic moment in this remaining term of the energy integral equation. Figure 6 (which also appears in Ref. 2) considers this question for a symmetric body, $C_{m_{2-}} = C_{m_{2+}}$. The ordinate is the ratio of the prime term of the energy integral equation calculated with equivalent cubic and linear moments, while the abscissa is the oscillation amplitude. The various curves represent different pitching moments from almost linear,
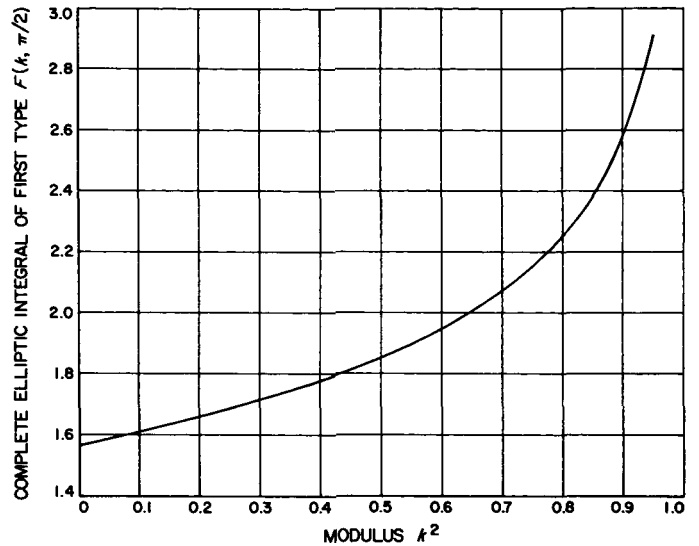
Fig. 5. Complete elliptic integral of the first kind vs elliptic modulus
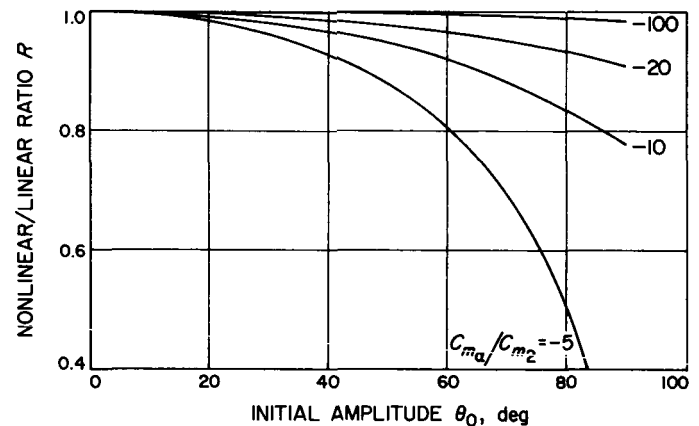
Fig. 6. Errors introduced by using a linear moment to approximate a cubic moment

$C_{m_\alpha}/C_{m_2} = -100$, to fairly nonlinear, $C_{m_\alpha}/C_{m_2} = -5$. As the figure shows, the error can become significant at the higher amplitudes. Although this plot concerns a symmetric body, the magnitudes of the errors are indicative of the asymmetric case.

Consider the integral,

$$\int_{-\theta_0}^{\theta_1} \theta' d\theta$$

Again, there are four possible cases corresponding to the combinations of the algebraic signs of $C_{m_{2-}}$ and $C_{m_{2+}}$. An example with $C_{m_{2-}} > 0$ and $C_{m_{2+}} < 0$ will be carried out.

The other three cases may be generated by symmetry from the results given.

$$\int_{-\theta_0}^{\theta_1} \theta' d\theta = (k_m C_{m_{2-}})^{\frac{1}{2}} \int_{-\theta_0}^{0} (\theta^2 - \theta_0^2)^{\frac{1}{2}} \left(\theta^2 + \frac{C_{m_\alpha}}{C_{m_{2-}}} + \theta_0^2\right)^{\frac{1}{2}} d\theta + (k_m C_{m_{2+}})^{\frac{1}{2}} \int_{0}^{\theta_1} (\theta^2 - \theta_1^2)^{\frac{1}{2}} \left(\theta^2 + \frac{C_{m_\alpha}}{C_{m_{2+}}} + \theta_1^2\right)^{\frac{1}{2}} d\theta$$

(59)

Let

$$k_-^2 = -\frac{\theta_0^2}{\dfrac{C_{m_\alpha}}{C_{m_{2-}}} + \theta_0^2}, \qquad \bar{k}_-^2 = 1 - k_-^2, \qquad k_+^2 = \frac{\theta_1^2}{\dfrac{C_{m_\alpha}}{C_{m_{2+}}} + 2\theta_1^2}, \qquad \bar{k}_+^2 = 1 - k_+^2, \qquad \phi_- = \sin^{-1}\frac{\theta}{\theta_0}, \qquad \phi_+ = \cos^{-1}\frac{\theta}{\theta_0}$$

Then,

$$\int_{-\theta_0}^{\theta_1} \theta' d\theta = \frac{(k_m)^{\frac{1}{2}}}{3} \left\{ (C_{m_{2-}})^{\frac{1}{2}} \left[-\left(\frac{C_{m_\alpha}}{C_{m_{2-}}} + \theta_0^2\right) \right]^{\frac{3}{2}} \left[(1 + k_-^2) E\left(k_-, \frac{\pi}{2}\right) - (1 - k_-^2) F\left(k_-, \frac{\pi}{2}\right) \right] \right.$$

$$\left. + (-C_{m_{2+}})^{\frac{1}{2}} \left(\frac{C_{m_\alpha}}{C_{m_{2-}}} + 2\theta_0^2\right)^{\frac{3}{2}} \left[(2k_+^2 - 1) E\left(k_+, \frac{\pi}{2}\right) + (1 - k_+^2) F\left(k_+, \frac{\pi}{2}\right) \right] \right\}$$

(60)

where $F(k, \phi)$ and $E(k, \phi)$ are the Legendre canonical forms of elliptic integrals of the first and second kinds, respectively. This can be rewritten as in Eq. (61), letting $G_1(k_-)$ and $G_2(k_+)$ have obvious denotations, as follows:

$$\int_{-\theta_0}^{\theta_1} \theta' d\theta = \frac{(k_m)^{\frac{1}{2}}}{3} \left[(C_{m_{2-}})^{\frac{1}{2}} \left(\frac{\theta_0}{k_-}\right)^3 G_1(k_-) + (C_{m_{2+}})^{\frac{1}{2}} \left(\frac{\theta_1}{k_+}\right)^3 G_2(k_+) \right]$$

(61)

For reference purposes, Fig. 7 shows G_1 and G_2 vs k^2.

When the results are collected, the dynamic stability derivative is given by

$$(C_{m_q} + C_{m_{\dot\alpha}}) \frac{md^2}{I} = \frac{\dfrac{md}{I}(C_{m_\alpha}\theta_1 + 2C_{m_{2+}}\theta_1^3)}{\displaystyle\int_{-\theta_0}^{\theta_1} \theta' d\theta} + \text{lift term} - \text{drag term}$$

(62)

where

$$\int_{-\theta_0}^{\theta_1} \theta' d\theta$$

is given by Eq. (61), lift term by Eq. (47), and drag term by Eq. (48).

E. Full-Cubic Pitching Moment

The cases considered in the previous sections were intended to afford some degree of nonlinearity to the problem, and yet to limit the complexity of the integrals and resulting solutions. More general functional forms for the pitching moment, e.g., an unrestricted power series expansion, could be handled with the same approach. However, as the series becomes longer the solution becomes difficult and the number of needed case distinction multiplies. Therefore, direct numerical integrations of Eqs. (25) and (27) rather than an analytical approach, seem more practical. To exemplify the difficulties which can arise, consider the following pitching moment:

$$C_m(\theta) = C_{m_\alpha}\theta + \frac{3}{2} C_{m_1}\theta^2 + 2C_{m_2}\theta^3$$
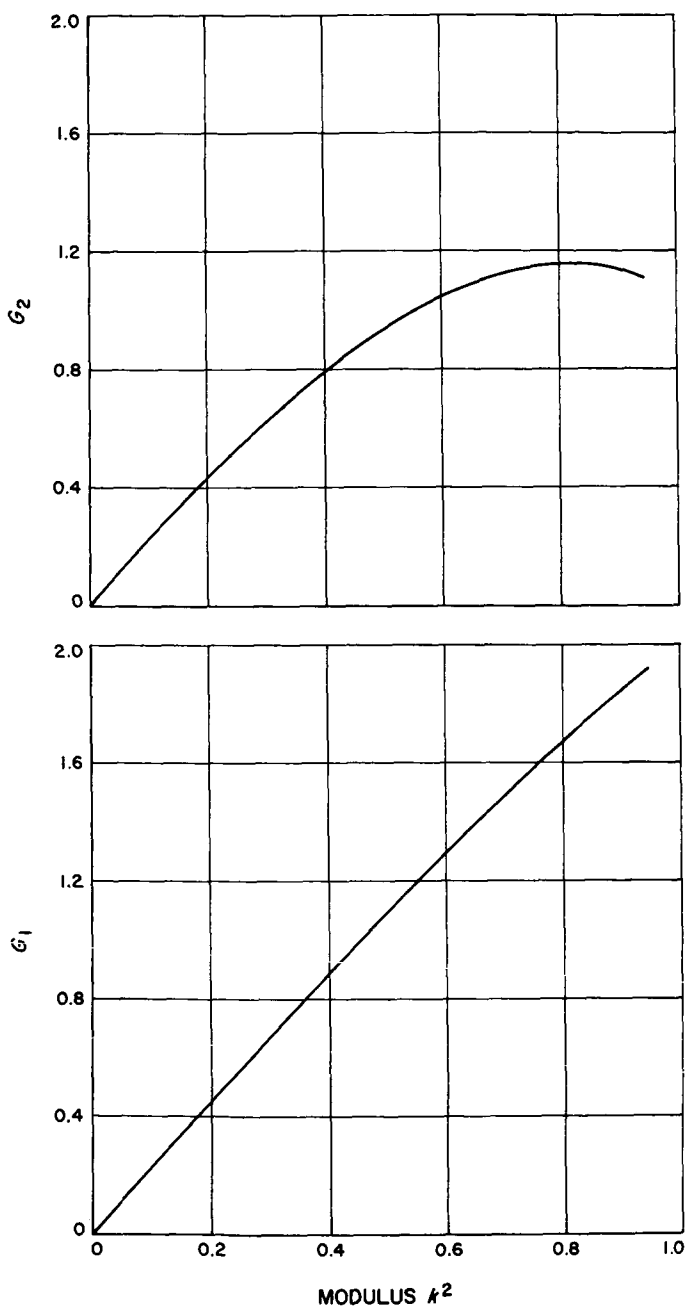
(63)

Fig. 7. The functions G_1 and G_2 vs elliptic modulus

This is the simplest power series representation available beyond the pitching moments considered previously. A closed-form solution in terms of tabulated functions is obtained; however, the solution is restricted to one of several possible case distinctions and is more complex than is desirable. This particular pitching moment may be considered as the longest power series expansion for which an analytical solution is practical.

1. Calculation of θ_1.

$$\int_{-\theta_0}^{\theta_1} C_m(\theta)\, d\theta = 0 = \frac{\theta_1^2}{2}\left(C_{m_\alpha} + C_{m_1}\theta_1 + C_{m_2}\theta_1^2\right)$$

$$-\frac{\theta_0^2}{2}\left(C_{m_\alpha} - C_{m_1}\theta_0 + C_{m_2}\theta_0^2\right)$$

or, rearranging

$$\theta_1^4 + \frac{C_{m_1}}{C_{m_2}}\theta_1^3 + \frac{C_{m_\alpha}}{C_{m_2}}\theta_1^2 - \left(\theta_0^4 - \frac{C_{m_1}}{C_{m_2}}\theta_0^3 + \frac{C_{m_\alpha}}{C_{m_2}}\theta_0^2\right) = 0 \tag{64}$$

One root of this equation must be $-\theta_0$ since

$$\int_{-\theta_0}^{-\theta_0} C_m(\theta)\, d\theta = 0$$

Dividing by $[\theta_1 - (-\theta_0)]$ results in a cubic equation for θ_1, as follows:

$$\theta_1^3 + \left(\frac{C_{m_1}}{C_{m_2}} - \theta_0\right)\theta_1^2 + \left(\frac{C_{m_\alpha}}{C_{m_2}} - \frac{C_{m_1}}{C_{m_2}}\theta_0 + \theta_0^2\right)\theta_1$$

$$-\left(\frac{C_{m_\alpha}}{C_{m_2}}\theta_0 - \frac{C_{m_1}}{C_{m_2}}\theta_0^2 + \theta_0^3\right) = 0 \tag{65}$$

An examination of the coefficients of this equation will reveal the following facts: (1) If C_{m_2} is positive, there are three real roots, two positive and one negative; (2) if C_{m_2} and C_{m_1} are both negative, there is only one real root and it is positive; (3) if C_{m_2} is negative and C_{m_1} is positive, there may be only one real root that is positive, or there may be three real roots, one positive and the other two either both positive or both negative. Over a large α range, the first case is the most likely physically; it is indicative of an initial increase in static stability with increasing α, and a subsequent leveling off and decrease in stability with further increase in angle. Because this is the most likely situation, the remainder of the discussion on this moment curve will be restricted to the first case.

The algebraic solution of Eq. (65) using Cardan's formulas (Ref. 9) is tedious and offers no simplification to the problem, as did the result for the bi-linear case. Therefore, expressions for the roots in terms of the coefficients will not be listed here. It is sufficient to say that the three roots of Eq. (65) may be obtained algebraically or by using a

simple iterative technique, such as the Newton-Raphson method (Ref. 10). For convenience, the Newton-Raphson method, as well as several other iterative techniques, are described in the Appendix. The oscillation amplitude peak θ_1 will be the smaller of the two positive roots. The other two roots of Eq. (65) are useful in upcoming integrations; therefore, assume this equation has been completely solved, either algebraically or numerically, for roots θ_1, θ_2, and $-\theta_3$ and that the following inequality holds: $-\theta_3 < -\theta_0 < 0 < \theta_1 < \theta_2$.

2. *Estimate of θ'.* By a direct application of Eq. (27),

$$\theta' = (k_m)^{\frac{1}{2}} [C_{m_\alpha}(\theta^2 - \theta_0^2) + C_{m_1}(\theta^3 + \theta_0^3) + C_{m_2}(\theta^4 - \theta_0^4)]^{\frac{1}{2}} \tag{66}$$

In light of the prior discussion on roots of Eq. (65), this can be written in the more convenient form,

$$\theta' = (k_m C_{m_2})^{\frac{1}{2}} [(\theta + \theta_3)(\theta + \theta_0)(\theta - \theta_1)(\theta - \theta_2)]^{\frac{1}{2}} \tag{67}$$

3. *Estimate of ½-cycle distance period, $X_{\frac{1}{2}}$.*

$$X_{\frac{1}{2}} = \frac{1}{(k_m C_{m_2})^{\frac{1}{2}}} \int_{-\theta_0}^{\theta_1} \frac{d\theta}{[(\theta + \theta_3)(\theta + \theta_0)(\theta - \theta_1)(\theta - \theta_2)]^{\frac{1}{2}}} \tag{68}$$

Let

$$k^2 = \frac{(\theta_1 + \theta_0)(\theta_2 + \theta_3)}{(\theta_2 + \theta_0)(\theta_1 + \theta_3)}, \qquad \phi = \sin^{-1}\left[\frac{(\theta_1 + \theta_3)(\theta + \theta_0)}{(\theta_1 + \theta_0)(\theta + \theta_3)}\right]^{\frac{1}{2}}$$

Then

$$X_{\frac{1}{2}} = \frac{2F\left(k, \dfrac{\pi}{2}\right)}{[k_m C_{m_2}(\theta_2 + \theta_0)(\theta_1 + \theta_3)]^{\frac{1}{2}}} \tag{69}$$

4. *Aerodynamic damping coefficient.* As in the bi-cubic case, the lift and drag contributions can be regarded as of secondary importance and approximated with an equivalent bi-linear moment. Therefore, we are, again, left with the following term:

$$\int_{\theta_0}^{\theta_1} \theta' \, d\theta = (k_m C_{m_{2+}})^{\frac{1}{2}} \int_{-\theta_0}^{\theta_1} [(\theta + \theta_3)(\theta + \theta_0)(\theta - \theta_1)(\theta - \theta_2)]^{\frac{1}{2}} \, d\theta \tag{70}$$

It is at this point that the value of the closed-form solution becomes questionable. By using the substitution

$$k^2 = \frac{(\theta_1 + \theta_0)(\theta_2 + \theta_3)}{(\theta_2 + \theta_0)(\theta_1 + \theta_3)}$$

$$\tilde{a}^2 = \frac{(\theta_1 + \theta_0)}{(\theta_1 + \theta_3)}, \qquad 0 < \tilde{a}^2 < k^2$$

$$\phi = \sin^{-1}\left[\frac{(\theta_1 + \theta_3)(\theta + \theta_0)}{(\theta_1 + \theta_0)(\theta + \theta_3)}\right]^{\frac{1}{2}}$$

Table 2. G_3 vs $\bar{\sigma}^2$ and k^2

Elliptic integral parameter $\bar{\sigma}^2$

Elliptic modulus k^2	0.00	0.05	0.10	0.15	0.20	0.25	0.30	0.35	0.40	0.45	0.50	0.55	0.60	0.65	0.70	0.75	0.80	0.85	0.90	0.91	0.92	0.93	0.94
0.00	0.0																						
0.05	0.0																						
0.10	0.0	0.0105	0.0129ª	0.0153	0.0177	0.0208																	
0.15	0.0	0.0104	0.0231	0.0259	0.0287	0.0312	0.0329																
0.20	0.0	0.0105	0.0229	0.0385	0.0420	0.0454	0.0486	0.0500															
0.25	0.0	0.0099	0.0226	0.0380	0.0572	0.0614	0.0656	0.0695	0.0719														
0.30	0.0	0.0098	0.0221	0.0373	0.0563	0.0803	0.0856	0.0909	0.0957	0.0981													
0.35	0.0	0.0095	0.0218	0.0367	0.0553	0.0787	0.1084	0.1148	0.1208	0.1253	0.1208												
0.40	0.0	0.0099	0.0216	0.0361	0.0543	0.0772	0.1065	0.1443	0.1525	0.1604	0.1670	0.1674											
0.45	0.0	0.0099	0.0211	0.0355	0.0533	0.0757	0.1044	0.1415	0.1905	0.2012	0.2118	0.2207	0.2223										
0.50	0.0	0.0087	0.0208	0.0348	0.0523	0.0742	0.1022	0.1384	0.1861	0.2500	0.2640	0.2773	0.2876	0.2816									
0.55	0.0	0.0090	0.0202	0.0340	0.0512	0.0726	0.0999	0.1352	0.1816	0.2440	0.3298	0.3490	0.3678	0.3836	0.3862								
0.60	0.0	0.0084	0.0197	0.0334	0.0501	0.0710	0.0976	0.1319	0.1769	0.2374	0.3206	0.4385	0.4650	0.4906	0.5100	0.4958							
0.65	0.0	0.0087	0.0195	0.0326	0.0489	0.0693	0.0951	0.1285	0.1721	0.2306	0.3109	0.4246	0.5916	0.6300	0.6671	0.6954	0.6751						
0.70	0.0	0.0092	0.0188	0.0319	0.0477	0.0675	0.0926	0.1249	0.1671	0.2235	0.3009	0.4100	0.5702	0.8165	0.8745	0.9312	0.9747	0.9422					
0.75	0.0	0.0090	0.0188	0.0310	0.0465	0.0657	0.0900	0.1212	0.1619	0.2162	0.2903	0.3948	0.5475	0.7817	1.1636	1.2570	1.3494	1.4210	1.3657				
0.80	0.0	0.0091	0.0182	0.0303	0.0452	0.0638	0.0873	0.1173	0.1564	0.2084	0.2792	0.3787	0.5236	0.7449	1.1041	1.7378	1.9008	2.0653	2.1953	2.0886			
0.85	0.0	0.0081	0.0177	0.0293	0.0438	0.0618	0.0844	0.1132	0.1506	0.2001	0.2674	0.3615	0.4980	0.7053	1.0401	1.6268	2.7833	3.1049	3.4418	3.7235	3.5309		
0.90	0.0	0.0084	0.0172	0.0284	0.0425	0.0597	0.0813	0.1088	0.1444	0.1913	0.2547	0.3430	0.4702	0.6623	0.9701	1.5048	2.5476	4.9820	5.7510	6.6119	7.4129	7.0804	
0.95	0.0	0.0078	0.0167	0.0276	0.0409	0.0574	0.0780	0.1040	0.1376	0.1816	0.2407	0.3225	0.4394	0.6142	0.8913	1.3662	2.2771	4.3576	10.8360	13.4390	16.8067	20.7772	21.7279

ªThe upper scale, $\bar{\sigma}^2$, does not apply to the entries to the right of the heavy black line. As $\bar{\sigma}^2$ approaches k^2, the function G_3 starts changing more radically, and intervals on $\bar{\sigma}^2$ of 0.05 are not adequate for interpolation and extrapolation. Therefore, the entries to the right of the heavy black line represent 0.01 intervals of $\bar{\sigma}^2$ from the last entry to the left of the heavy black line in each row. For example, in the row corresponding to $k^2 = 0.65$, the footnoted entries are for values of $\bar{\sigma}^2$ equal to 0.61, 0.62, 0.63, and 0.64.

the following solution results:

$$\int_{-\theta_0}^{\theta_1} \theta' \, d\theta = 2\frac{(k_m C_{m_{2+}})^{\frac{1}{2}} (\theta_2 + \theta_0)(\theta_1 + \theta_0)(\theta_3 - \theta_0)^2}{[(\theta_2 + \theta_0)(\theta_1 + \theta_3)]^{\frac{1}{2}}} G_3 (\tilde{a}^2, k^2)$$ (71)

where

$$G_3 (\tilde{a}^2, k^2) = \frac{1}{\tilde{a}^4}\left[-k^2 \Pi \left(\frac{\pi}{2}, \tilde{a}^2, k \right) + (3k^2 - \tilde{a}^2 k^2 - \tilde{a}^2) V_2 + (2\tilde{a}^2 k^2 + 2\tilde{a}^2 - 3k^2 - \tilde{a}^4) V_3 + (\tilde{a}^2 - 1)(\tilde{a}^2 - k^2) V_4 \right]$$

$$V_2 = \frac{1}{2(\tilde{a}^2 - 1)(k^2 - \tilde{a}^2)}\left[\tilde{a}^2 E \left(k, \frac{\pi}{2} \right) + (k^2 - \tilde{a}^2) F \left(k, \frac{\pi}{2} \right) + (2\tilde{a}^2 k^2 + 2\tilde{a}^2 - 3k^2 - \tilde{a}^4) \Pi \left(\frac{\pi}{2}, \tilde{a}^2, k \right) \right]$$

$$V_3 = \frac{1}{4(1 - \tilde{a}^2)(k^2 - \tilde{a}^2)}\left[k^2 F \left(k, \frac{\pi}{2} \right) + 2(\tilde{a}^2 k^2 + \tilde{a}^2 - 3k^2) \Pi \left(\frac{\pi}{2}, \tilde{a}^2, k \right) + 3(\tilde{a}^4 + 3k^2 - 2\tilde{a}^2 k^2 - 2\tilde{a}^2) V_2 \right]$$

$$V_4 = \frac{1}{6(1 - \tilde{a}^2)(k^2 - \tilde{a}^2)}\left[3k^2 \Pi \left(\frac{\pi}{2}, \tilde{a}^2, k \right) + 4(\tilde{a}^2 k^2 + \tilde{a}^2 - 3k^2) V_2 + 5(\tilde{a}^4 + 3k^2 - 2\tilde{a}^2 k^2 - 2\tilde{a}^2) V_3 \right]$$

and $F(k, \pi/2)$, $E(k, \pi/2)$ and $\Pi(\pi/2, \tilde{a}^2, k)$ are complete elliptic integrals of the first, second, and third kinds, respectively. The dynamic stability derivative is, therefore, given by the following:

$$(C_{m_q} + C_{m_{\dot{\alpha}}})\frac{md^2}{I} = \frac{\frac{md}{I}\delta\theta \left(C_{m_\alpha}\theta_1 + \frac{3}{2}C_{m_1}\theta_1^2 + 2C_{m_2}\theta_1^3 \right)(\theta_1 + \theta_3)^{\frac{1}{2}}}{2[k_m C_{m_2}(\theta_2 + \theta_0)]^{\frac{1}{2}}(\theta_1 + \theta_0)(\theta_3 - \theta_0)^2 G_3 (a^2, k^2)}$$

$$+ \text{ lift term} - \text{drag term}$$ (72)

As can be seen, this is not an easy solution to apply to experimental data. For convenience, the function $G_3 (\tilde{a}^2, k^2)$ is tabulated vs $\tilde{a}^2$ and k^2 in Table 2. Even with this aid, the solution (though workable) is not simple and represents only one (the most likely one) of the possible case distinctions. Furthermore, a numerical approach has been suggested for obtaining the angles θ_1, θ_2, and θ_3. Therefore, it can be concluded that perhaps for this moment (and certainly for any pitching moment with a longer power series representation) either an approximating moment curve or numerical integrations must be used.

III. Equivalence Relations Between Moment Curves

A. Equivalence Criteria

The previous sections of this report have noted that there are a limited number of pitching moment representations for which closed-form solutions are feasible. These include the offset linear, bi-linear, bi-cubic, and, possibly, the full-cubic moments that were discussed in Sections II-B to II-E. If we are given an arbitrary body, its pitching moment curve generally would not conform exactly to

one of these representations. Therefore, if an analytical solution for the damping coefficient is desired, the actual pitching moment must be approximated with one of these four curves. This section deals with a method of determining the coefficients of an approximating moment curve.

Assume that an arbitrary pitching moment curve is given in either tabulated or functional form. An approximating functional moment could be determined through use of conventional curve-fitting methods, such as the least-squares technique. However, with such an approach, although the approximating moment would be in some sense close to the original curve, there would be no assurance that any of the motion characteristics corresponding to these two curves actually would be the same. A better approach would be to use the matching of important parameters of motion as the requirement for the selection of the coefficients of the approximating moment curve. The offset linear and bi-linear moments each have two coefficients, and thus *two* characteristics of the angular motion can be matched. The bi-cubic and full-cubic moments each have three coefficients and allow the equating of three motion parameters.

The first (and most important) characteristic to match is the ½-cycle distance oscillation period, $X_{\frac{1}{2}}$. In actual application, an average value of the decay per ½ cycle, $\delta\theta$, will be determined over several cycles of motion. It is, therefore, necessary that the angular oscillations corresponding to the original and approximating moment curves remain in phase over this region of application. The second criterion is to match the amplitude peaks of the non-dissipative angular motion, i.e., given the initial angle $-\theta_0$, the corresponding positive peak θ_1 should be the same for both moments. Matching of only these two conditions ensures great similarity between the motions, and will be the criteria used to determine the coefficients of an equivalent offset linear or bi-linear pitching moment. One more condition is available if either of the cubic moments is used on the approximating curve. Because the angular velocity θ' appears as a weighting factor of the dynamic stability derivative in the differential equation of motion, it would seem desirable to have similar angular velocity histories over the ½ cycle. This is borne out by the fact that in the energy integral equation, the most critical term is

$$\int_{-\theta_0}^{\theta_1} \theta' \, d\theta$$

The second condition above ensures that the angular velocities will be identical (i.e., equals 0) at least two points during the ½ cycle, $-\theta_0$ and at θ_1. Furthermore, the matching of the ½-cycle distance periods suggests that the angular velocity histories are of similar nature. The additional degree of freedom afforded by the cubic moments will be used to match the maximum angular velocity over the ½-oscillation cycle, i.e., the angular velocity as the vehicle passes through zero angle-of-attack. These three conditions will then ensure a very good approximating representation of the original moment curve.

The actual mechanics of determining the approximating moment curve depend on the knowledge of the true pitching moment. It can be assumed that the original pitching moment is given either as a functional form, say a finite power series expansion, or as a tabulation. The polynomial representation may always be integrated directly, as indicated by Eq. (27), to yield θ' as a function of θ and θ_0. By setting $\theta = 0$ in this expression, the maximum angular velocity, $\theta'_{\max}$, as a function of θ_0 is obtained. An alternative method to determine this quantity, which does not require a functional form for the original pitching moment, would be to numerically differentiate the experimental angular history at $\theta = 0$. However, the use of this technique imposes more stringent sampling frequency and accuracy requirements on the experimental data. The result of the integration mentioned can also be used to obtain θ_1, the positive amplitude peak. At this point, the angular velocity will have to be zero. Then, θ_1 is the smallest positive root to the equation $\theta' = 0$. This step can also be performed without actually knowing a functional representation for the pitching moment. A tabular form of the moment may be integrated mechanically or numerically, and the result used to determine θ_1. Finally, the ½-cycle distance period $X_{\frac{1}{2}}$ and the initial amplitude $-\theta_0$ may be obtained directly from the free-flight trajectory. These four quantities, $\theta'_{\max}$, $-\theta_0$, θ_1, and $X_{\frac{1}{2}}$ will be used to determine the approximating moment curve. Most of the necessary derivations have already been done in Section II. The following sections consist of manipulation of previous equations and statements of results.

B. Offset Linear and Bi-Linear Pitching Moments

1. Offset linear pitching moment: $C_m(\theta) = C_{m_0} + C_{m_\alpha}\theta$. Equations (33) and (36) provide the solutions for C_{m_0} and C_{m_α}, as follows:

$$C_{m_\alpha} = -\pi^2/k_m (X_{\frac{1}{2}})^2 \tag{73}$$

$$C_{m_0} = \left(\frac{\theta_0 - \theta_1}{2}\right) C_{m_\alpha} \tag{74}$$

2. Bi-linear pitching moment:

$$C_m(\theta) = C_{m_{\alpha-}}\theta; \qquad \theta \leq 0$$

$$C_m(\theta) = C_{m_{\alpha+}}\theta; \qquad \theta \geq 0$$

Rearrangement of Eqs. (43) and (45) yields the following:

$$C_{m_\alpha} = \frac{1}{k_m}\left[\pi/2 \frac{(1 + \theta_1/\theta_2)}{X_{\frac{1}{2}}}\right]^2 \tag{75}$$

$$C_{m_{\alpha+}} = C_{m_\alpha} \frac{\theta_0^2}{\theta_1^2} \tag{76}$$

C. Bi-Cubic Pitching Moment

$$C_m(\theta) = C_{m_\alpha}\theta + 2C_{m_{2-}}\theta^3; \qquad \theta \leq 0$$

$$C_m(\theta) = C_{m_\alpha}\theta + 2C_{m_{2+}}\theta^3; \qquad \theta \geq 0$$

In the previous two cases, an actual calculation of the approximating moment curve was not necessary. The solutions for the damping coefficients, as given by Eqs. (37), (38), (39), (46), (47), and (48), are written in terms of the trajectory characteristics and do not explicitly involve the pitching moment. However, this is not the situation for the bi-cubic representation. The solution for the damping derivative involves the pitching moment both explicitly and implicitly in the moduli of the elliptic integrals. Therefore, it is necessary to produce the approximating moment curve. Furthermore, because of the implicit dependence through the elliptic integrals, the determining equations cannot be inverted directly to yield C_{m_α}, $C_{m_{2-}}$, and $C_{m_{2+}}$, but rather an iterative approach must be used. From Eq. (51) and from setting $\theta = 0$ in (53) or (54) to yield an expression for θ'_{max},

$$C_{m_{2+}} = C_{m_\alpha} \left(\frac{\theta_0^2 - \theta_1^2}{\theta_1^4} \right) + C_{m_{2-}} \frac{\theta_0^4}{\theta_1^4} \qquad (77)$$

$$C_{m_\alpha} = -\frac{(\theta'_{max})^2}{k_m \theta_0^2} - C_{m_{2-}} \theta_0^2 = -\frac{(\theta'_{max})^2}{k_m \theta_1^2} - C_{m_{2+}} \theta_1^2 \qquad (78)$$

Instead of iterating on three equations in three unknowns, it is more expedient to solve the above two equations for two of the variables in terms of the remaining one, and then use the third equation to develop a recursion formula. Combining Eqs. (77) and (78) and rearranging

$$C_{m_{2+}} = -\frac{(\theta'_{max})^2}{k_m \theta_0^2} \frac{(\theta_0^2 - \theta_1^2)}{\theta_1^4} + \frac{\theta_0^2}{\theta_1^2} C_{m_{2-}} \qquad (79)$$

The third equation involves the ½-distance period $X_{\frac{1}{2}}$ and, therefore, will vary according to the algebraic signs of the cubic terms. A good estimate of the proper signs may be obtained by an inspection of the concavity characteristics of the moment curve. A precise method to determine the existence of a solution under the assumption of a particular combination of signs is available through the two inequalities $0 < k_-^2 < 1$ and $0 < k_+^2 < 1$. The elliptic moduli, k_-^2 and k_+^2 may be written in terms of one unknown, say $C_{m_{2-}}$, with the aid of Eqs. (78) and (79). Simplifying will result in inequalities imposing conditions relating the angles θ_0 and θ_1. This is to be expected, i.e., the shape of the approximating moment curve would depend on the angles it must pass through when inscribing zero area. In general, more than one solution may exist; however, all should be equally valid, and it is the experimenter's choice which to use. The inequalities which comprise this existence test are derived in the succeeding paragraphs.

The simplest iterative procedure to use is different, depending on whether cubic coefficients are positive or whether at least one is negative. For a body with positive lift at zero angle-of-attack, it is likely that the restoring moment is less in magnitude at a given negative angle-of-attack than it is at the positive angle equal in absolute value. This means that $C_{m_{2-}}$ is destabilizing, i.e., positive. The two cases with $C_{m_{2-}} > 0$ are discussed here. The remaining two cases, $C_{m_{2-}} < 0$, could be handled similarly.

1. $C_{m_{2-}} > 0$, $C_{m_{2+}} > 0$. From Table 1 we get the following:

$$X_{\frac{1}{2}} = \frac{1}{(k_m)^{\frac{1}{2}}} \left[\left(-\frac{1}{C_{m_\alpha} + C_{m_{2-}} \theta_0^2} \right)^{\frac{1}{2}} F \left(k_-, \frac{\pi}{2} \right) \right.$$
$$\left. + \left(-\frac{1}{C_{m_\alpha} + C_{m_{2+}} \theta_1^2} \right)^{\frac{1}{2}} F \left(k_+, \frac{\pi}{2} \right) \right] \qquad (80)$$

where

$$k_-^2 = -C_{m_{2-}} \theta_0^2 / (C_{m_\alpha} + C_{m_{2-}} \theta_0^2)$$

$$k_+^2 = -C_{m_{2+}} \theta_1^2 / (C_{m_\alpha} + C_{m_{2+}} \theta_1^2)$$

By using Eqs. (78) and (79),

$$X_{\frac{1}{2}} - \frac{\theta_0}{\theta'_{max}} F \left(k_-, \frac{\pi}{2} \right) - \frac{\theta_1}{\theta'_{max}} F \left(k_+, \frac{\pi}{2} \right) = 0 \qquad (81)$$

where

$$k_-^2 = \frac{C_{m_{2-}} k_m \theta_0^4}{(\theta'_{max})^2}$$

$$k_+^2 = -\frac{(\theta_0^2 - \theta_1^2)}{\theta_0^2} + \frac{\theta_0^2 \theta_1^2 k_m}{(\theta'_{max})^2} C_{m_{2-}}$$

Examining the two inequalities implied by the elliptic moduli, the condition needed for this case to be applicable is as follows:

$$\frac{1}{2} < \frac{\theta_0^2}{\theta_1^2} < 2 \qquad \text{or} \qquad 0.707 < \frac{\theta_0}{\theta_1} < 1.414$$

The Newton-Raphson method is well suited for Eq. (81), for example: Let

$$G\left(C_{m_{2-}}\right) = X_{\frac{1}{2}} - \frac{\theta_0}{\theta'_{max}} F\left(k_-, \frac{\pi}{2}\right) - \frac{\theta_1}{\theta'_{max}} F\left(k_+, \frac{\pi}{2}\right)$$

then

$$\frac{dG}{dC_{m_{2-}}} = -\frac{\theta_0}{\theta'_{max}} \frac{dF\left(k_-, \frac{\pi}{2}\right)}{dk} \frac{dk_-}{dC_{m_{2-}}} - \frac{\theta_1}{\theta'_{max}} \frac{dF\left(k_+, \frac{\pi}{2}\right)}{dC_{m_{2-}}} \tag{82}$$

where

$$\frac{dF\left(k, \frac{\pi}{2}\right)}{dk} = \frac{E\left(k, \frac{\pi}{2}\right) - (1 - k^2) F\left(k, \frac{\pi}{2}\right)}{k(1 - k^2)}$$

$$\frac{dk_-}{dC_{m_2}} = \frac{k_m \theta_0^1}{2(\theta'_{max})^2 k_-}, \qquad \frac{dk_+}{dC_{m_2}} = \frac{\theta_0^2 \theta_1^2 k_m}{2(\theta'_{max})^2 k_+}$$

The recursion formula is as follows:

$$\left(C_{m_{2-}}\right)_{i+1} = \left(C_{m_{2-}}\right)_i - \frac{G\left(C_{m_{2-i}}\right)}{dG\left(C_{m_{2-i}}\right)/dc_{m_{2i}}} \tag{83}$$

Experience has shown that this iteration will, in general, converge rapidly, independent of the starting value.

2. $C_{m_{2-}} > 0, C_{m_{2+}} < 0$. From Table 1 and the previous section, we get

$$X_{\frac{1}{2}} = \frac{1}{(k_m)^{\frac{1}{2}}} \left[\frac{(k_m \theta_0)^{\frac{1}{2}}}{\theta'_{max}} F\left(k_-, \frac{\pi}{2}\right) + \left(-\frac{1}{C_{m_\alpha} + 2C_{m_{2+}} \theta_1^2}\right)^{\frac{1}{2}} F\left(k_+, \frac{\pi}{2}\right) \right] \tag{84}$$

where

$$k_-^2 = \frac{k_m \theta_0^4 C_{m_{2-}}}{(\theta'_{max})^2}; \qquad k_+^2 = \frac{C_{m_{2+}} \theta_1^2}{C_{m_\alpha} + 2C_{m_{2+}} \theta_1^2}$$

By using Eqs. (78) and (79)

$$X_{\frac{1}{2}} - \frac{\theta_0}{\theta'_{max}} F\left(k_-, \frac{\pi}{2}\right) - \left[\frac{\theta_1^2 \theta_0^2}{(2\theta_0^2 - \theta_1^2)(\theta'_{max})^2 - k_m \theta_1^2 \theta_0^4 C_{m_2}} \right]^{\frac{1}{2}} F\left(k_+, \frac{\pi}{2}\right) = 0 \tag{85}$$

where k^2 is as above and

$$k_+^2 = \frac{(\theta_0^2 - \theta_1^2)(\theta'_{max})^2 - k_m \theta_1^2 \theta_0^4 C_{m_2}}{(2\theta_0^2 - \theta_1^2)(\theta'_{max})^2 - k_m \theta_1^2 \theta_0^4 C_{m_{2-}}}$$

Again, from examining the elliptic moduli, the condition for applicability is $0 < \theta_1/\theta_0 < 1$. Combining this with the previous inequality, it follows that two solutions exist if

$$1 < \frac{\theta_0}{\theta_1} < 1.414$$

Employing the Newton-Raphson method to solve Eq. (73) would require a derivative with respect to $C_{m_{2-}}$, and would lead to a very complex recursion formula. A suggested approach is one which does not involve derivatives such as the method of accelerated iteration (see the Appendix) or perhaps a trial and error interval halving technique. Once a value for $C_{m_{2-}}$ is obtained, it may be substituted in Eqs. (77) and (78) to calculate C_{m_α} and $C_{m_{2+}}$.

D. Cubic Pitching Moment: $C_m(\theta) = C_{m_\alpha}\theta + 3/2\, C_{m_1}\theta^2 + 2C_{m_2}\theta^3$

The solution for the ½ cycle distance period again involves an elliptic integral and, therefore, an iterative approach is required. From Eqs. (64) and (66) we get the following:

$$C_{m_1} = -C_{m_\alpha}\left(\frac{\theta_1^2 - \theta_0^2}{\theta_1^3 + \theta_0^3}\right) - C_{m_2}\left(\frac{\theta_1^4 - \theta_0^4}{\theta_1^3 + \theta_0^3}\right) \tag{86}$$

$$C_{m_\alpha} = -\frac{(\theta'_{max})^2}{k_m \theta_0^2} + C_{m_1}\theta_0 - C_{m_2}\theta_0^2 \tag{87}$$

By using the latter two equations to solve for C_{m_α} and C_{m_1} in terms of C_{m_2} we obtain:

$$C_{m_\alpha} = -\frac{1}{k_m}\left(\frac{\theta'_{max}}{\theta_0\theta_1}\right)^2 (\theta_1^2 - \theta_0\theta_1 + \theta_0^2) - C_{m_2}\theta_0\theta_1 \tag{88}$$

$$C_{m_1} = \frac{1}{k_m}\left(\frac{\theta'_{max}}{\theta_0\theta_1}\right)^2 (\theta_1 - \theta_0) - C_{m_2}(\theta_1 - \theta_0) \tag{89}$$

The distance period equation involves the auxiliary angles θ_2 and θ_3. Two of the roots to Eq. (64) are known *a priori*, namely $-\theta_0$ and θ_1. A division then results in a quadratic for θ_2 and θ_3, as follows:

$$\theta^2 + \left[\frac{C_{m_1} - C_{m_2}(\theta_0 - \theta_1)}{C_{m_2}}\right]\theta + \frac{C_{m_\alpha} - C_{m_1}(\theta_0 - \theta_1) + C_{m_2}(\theta_0^2 - \theta_0\theta_1 + \theta_1^2)}{C_{m_2}} = 0 \tag{90}$$

By using Eqs. (88) and (89) to eliminate C_{m_α} and C_{m_1} from this quadratic, we get the following:

$$C_{m_2}\theta^2 + \left[\frac{1}{k_m}\left(\frac{\theta'_{max}}{\theta_0\theta_1}\right)^2 (\theta_1 - \theta_0)\right]\theta - \frac{1}{k_m}\left(\frac{\theta'_{max}}{\theta_0\theta_1}\right)^2 \theta_1\theta_0 = 0 \tag{91}$$

$$\theta_2, -\theta_3 = \frac{\frac{1}{k_m}\left(\frac{\theta'_{max}}{\theta_0\theta_1}\right)^2(\theta_0 - \theta_1) \pm \left\{\left[\frac{1}{k_m}\left(\frac{\theta'_{max}}{\theta_0\theta_1}\right)^2(\theta_0 - \theta_1)\right]^2 + \frac{4C_{m_2}}{k_m}\left(\frac{\theta'_{max}}{\theta_0\theta_1}\right)^2 \theta_1\theta_0\right\}^{1/2}}{2C_{m_2}} \tag{92}$$

The third equation is given by Eq. (69), as follows:

$$C_{m_2} - \left[\frac{2F\left(k, \frac{\pi}{2}\right)}{X_{\frac{1}{2}}}\right]^2 \frac{1}{k_m\left(\theta_2 + \theta_0\right)\left(\theta_1 + \theta_3\right)} = 0 \qquad (93)$$

where

$$k^2 = \frac{\left(\theta_1 + \theta_0\right)\left(\theta_2 + \theta_3\right)}{\left(\theta_2 + \theta_0\right)\left(\theta_1 + \theta_3\right)}$$

Again, to avoid complicated derivatives, accelerated iteration or an interval halving approach can be used with Eqs. (92) and (93) to obtain C_{m_2}. C_{m_α} and C_{m_1} may then be calculated from Eqs. (88) and (89).

IV. Applications and Accuracies

A. Approach

To exemplify the use of the formulas, and to verify their validity and accuracy, two sample cases have been worked out. The procedure employed was as follows: A six-degree-of-freedom computer program with aerodynamic coefficients as tabular inputs was used to simulate a wind-tunnel free-flight trajectory. Each of the four pitching moment curves discussed in this report was used as an approximating moment for analysis. Damping coefficients were calculated from the trajectory data corresponding to several initial amplitudes $-\theta_0$. A comparison between the resulting values and the input value of $(C_{m_q} + C_{m_{\dot\alpha}})$ is a direct measure of the accuracy of the equations.

The aerodynamics for the two computed cases were chosen particularly to provide a severe test for the data reduction formulas. Both sets of static coefficients are very nonlinear and very asymmetrical. The curves are realistic because they are similar to proposed hypersonic lifting re-entry bodies; however, rather than being representative of such a class of configurations, they are more than typically nonlinear in their static aerodynamics.

For the first sample case, the static pitching moment is given by the cubic representation of Section II-E. The primary reason for using this exact representation was to provide a direct verification of the validity of the cubic analysis. The second sample case represents what may be considered as an arbitrary pitching moment curve, given only in tabulated form. The distance period and maximum angular velocity histories were obtained directly from the simulated trajectory. The positive envelope peaks θ, cor-

responding to the initial angles $-\theta_0$, were obtained from a plotted moment curve with the aid of a planimeter. This sample case illustrates the application of the analysis in the most general possible circumstances, i.e., when a functional representation of the pitching moment is not given.

B. Sample Case 1

Consider a vehicle with static aerodynamic coefficients, as shown in Fig. 8, and an effective constant dynamic stability coefficient of -1.0. The static pitching moment adheres to a cubic representation with $C_{m_\alpha} = -0.1243$, $C_{m_1} = -0.1471$, and $C_{m_2} = 0.0678$. Using the solution presented in Section II-E, the majority of the analysis may be done parametrically, vs initial angle $-\theta_0$, without actually using experimental data. This means that for a given pitching moment curve, all but the determination of, and multiplication by, $\delta\theta$ need be done only once, and can be completed prior to an experimental test program.
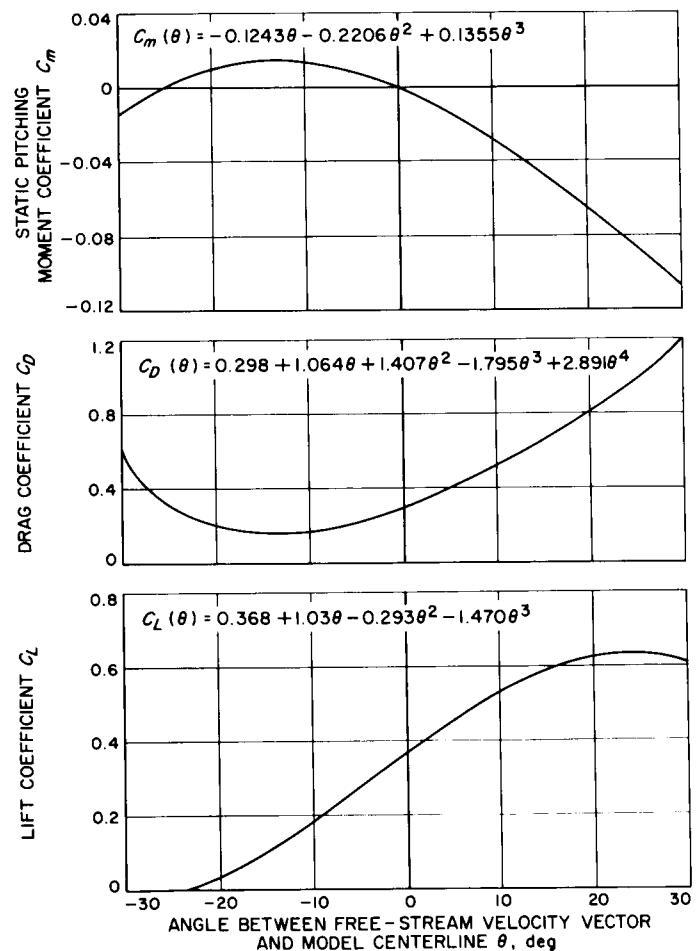

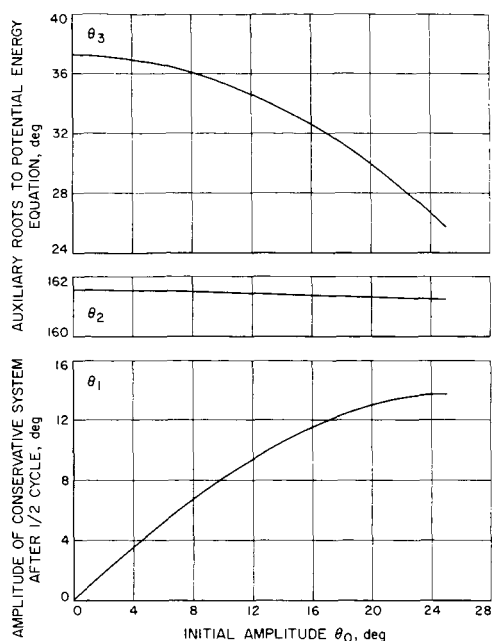Fig. 8. Static aerodynamics for sample case 1

Fig. 9. Roots of the potential energy equation for sample case 1

Fig. 11. Trajectory characteristics for sample case 1

Figure 9 shows the roots of Eq. (65), the potential energy equation, for this pitching moment. Shown is θ_1, the positive amplitude peak corresponding to a negative peak $-\theta_0$, θ_2, and $-\theta_3$ are the other auxiliary roots used in subsequent integrations. Figure 10 shows the two elliptic integral parameters, $\tilde{a}^2$ and k^2, vs θ_0. These curves, in a sense, provide a measure of the nonlinearity of the pitching moment. The larger the value of k^2 (i.e., the nearer to 1) and the closer $\tilde{a}^2$ is to k^2, the greater the nonlinearity of the problem. For this example, k^2 increases rapidly with θ_0, and $\tilde{a}^2$ is always close to k^2, therefore, indicating a very nonlinear pitching moment.
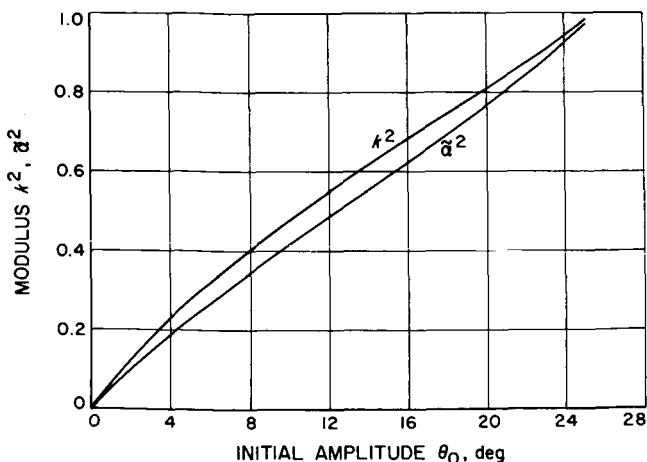
The maximum angular velocity $\theta'_{\max}$ and the ½-cycle oscillation period $X_{\frac{1}{2}}$ are plotted vs θ_0 in Fig. 11. The dashed lines result from Eqs. (67) and (69) while the solid lines are from the computer-calculated trajectory. There is excellent agreement between the numerical and analytical solutions at all amplitudes. These trajectory characteristics are not actually needed to calculate the damping derivative. They do, however, provide a standard of comparison for the various parts of the solution, and they become necessary later in the determination of approximate pitching moments.
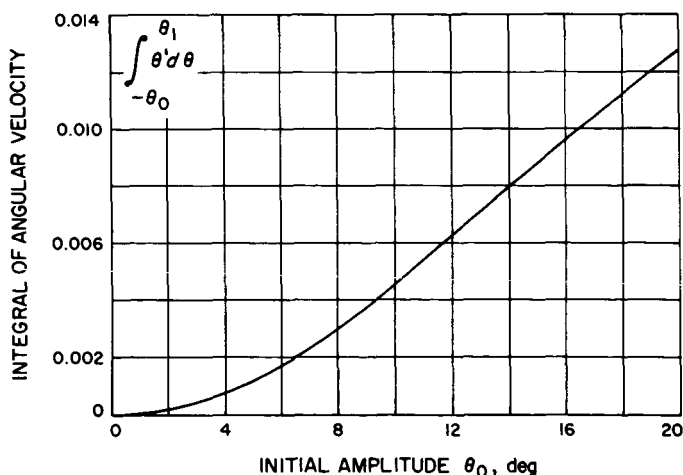

Fig 10. Elliptic integral parameters for sample case 1

Fig. 12. Integral of θ' for sample case 1

Figure 12 shows the integral of θ' over ½ of an oscillation cycle. This term comes from Eq. (71) in conjunction with Table 2. Finally, Fig. 13 shows the lift and drag terms vs θ_0 as calculated by Eqs. (47) and (48). Figures 8, 9, 12, and 13 may be used together with an experimental angular history to calculate dynamic stability derivatives.
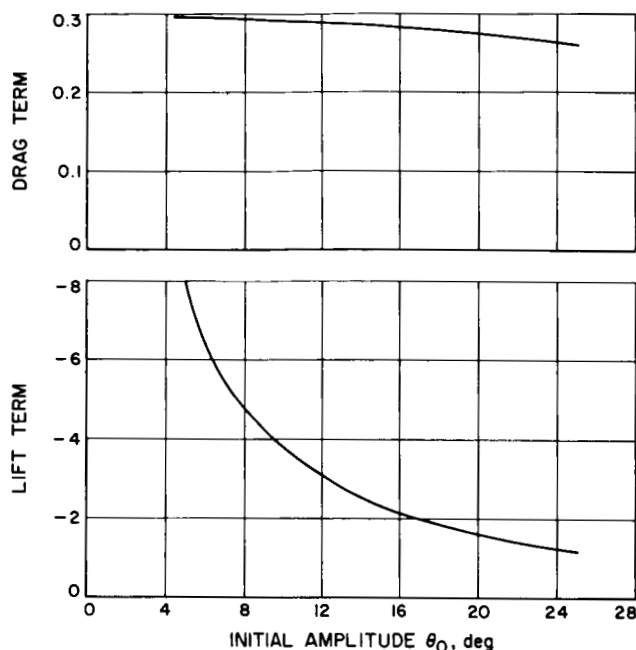

Fig. 13. Lift and drag terms for sample case 1

Figure 14 shows a computer-calculated trajectory for this sample case. This figure points out a difficulty that may arise when dealing with a high-lift configuration. Because the lift is always positive, rather than of alternating sign as in the case of a symmetric body, the velocity in the Z direction increases steadily throughout the flight. Late in the flight (say during the sixth oscillation cycle), the angle $(\theta - \alpha)$ has increased to about 1½ deg because of this Z velocity. An angle of this magnitude after a ½-oscillation cycle would not lead to difficulties because it has been adequately accounted for. However, considering the sixth cycle, itself, this term now enters as an initial condition $(\theta - \alpha)_0$, which previously was assumed to be zero. The result is a smaller decay than would otherwise be expected when oscillating from a negative to a positive peak, and a larger decay when oscillating in the other direction. This, in itself, suggests a method to correct for this possible error. The decay in both oscillatory directions may be measured—an equivalent amount of decay at the positive peak corresponding to the observed decay at the negative peak determined from Fig. 9—and this equivalent decay averaged with the other observed decay to give an
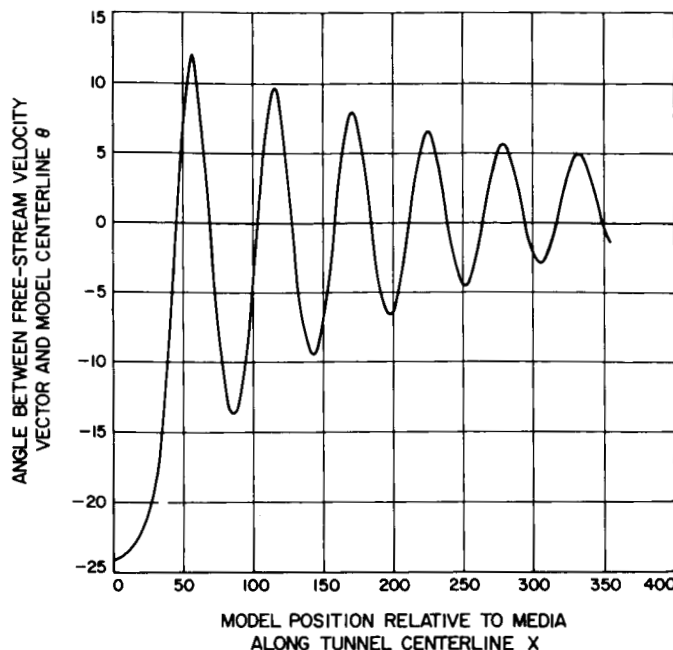

Fig. 14. Six-degree-of-freedom angular history, sample case 1

effective value corresponding to an average θ_0. This has been done for this particular trajectory, and the decay values were used in Eq. (72) to calculate damping coefficients. The numerical results are presented in the first three columns of Table 3. The agreement with the input value of $(C_{m_q} + C_{m_{\dot{\alpha}}}) = -1.0$ is excellent, within 1%, for all amplitudes considered. It must be noted, however, that the computer-determined decay, though rounded to the nearest 0.05 deg, is more accurate than could be determined from a wind-tunnel test. In actual practice, a good procedure to follow would be to plot the positive and negative peaks, fair smooth curves through the plotted data, and determine the decay from the smooth curves. The decay could be plotted vs θ_0 and smoothed again. With present data-gathering techniques, the result would probably be correct within 0.1 to 0.2 deg. This error in the determination of the decay would, of course, result in additional error in the final answer, the magnitude of which would depend on the actual level of the decay.

For comparison purposes, this trajectory has been analyzed assuming approximating pitching moments of the other three forms discussed in this report. For the offset linear and bi-linear moments, the damping derivatives can be calculated directly using Eqs. (37), (38), (39), (46), (47), and (48) without actually determining the approximating curve. The same is not true for the bi-cubic representation. Using the method outlined in Section III-C, the terms C_{m_α}, $C_{m_{\dot{\alpha}}}$, and $C_{m_{\dot{\alpha}+}}$ have been determined as functions of

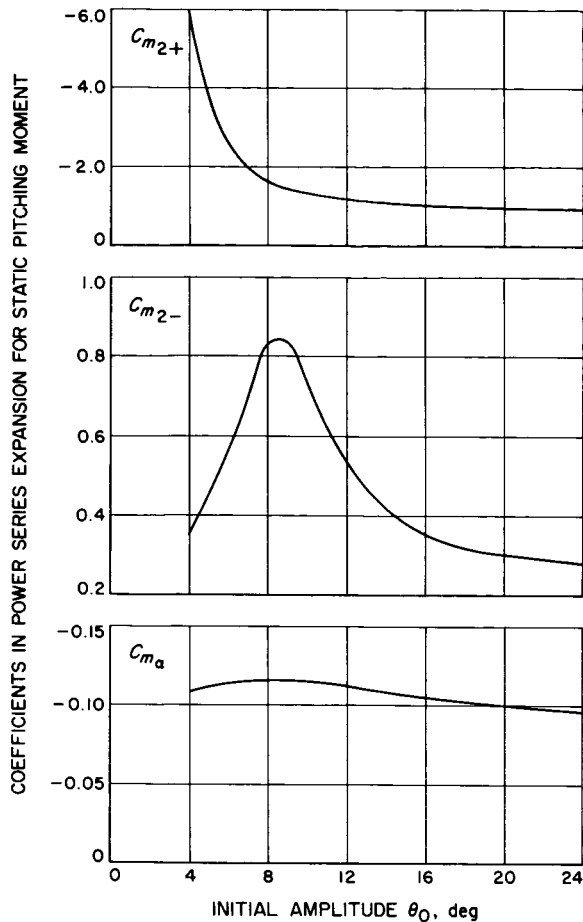Fig. 15. Equivalent bi-cubic pitching moment, sample case 1

Fig. 16. Static aerodynamics for sample case 2

θ_0, and are shown in Fig. 15. Then, Eq. (62) was used to calculate $(C_{m_q} + C_{m_{\dot{\alpha}}})$. The results for these three approximating moments are listed in Columns 4, 5, and 6 of Table 3. The accuracy with the bi-cubic approximations remains fairly good, with the maximum deviation on the order of 10%. However, the two linear approximations fall off in accuracy rather badly, with the error approaching 40% in the worst case. The sample case, then, emphasizes the need for a nonlinear analysis when the pitching moment is indeed quite nonlinear.
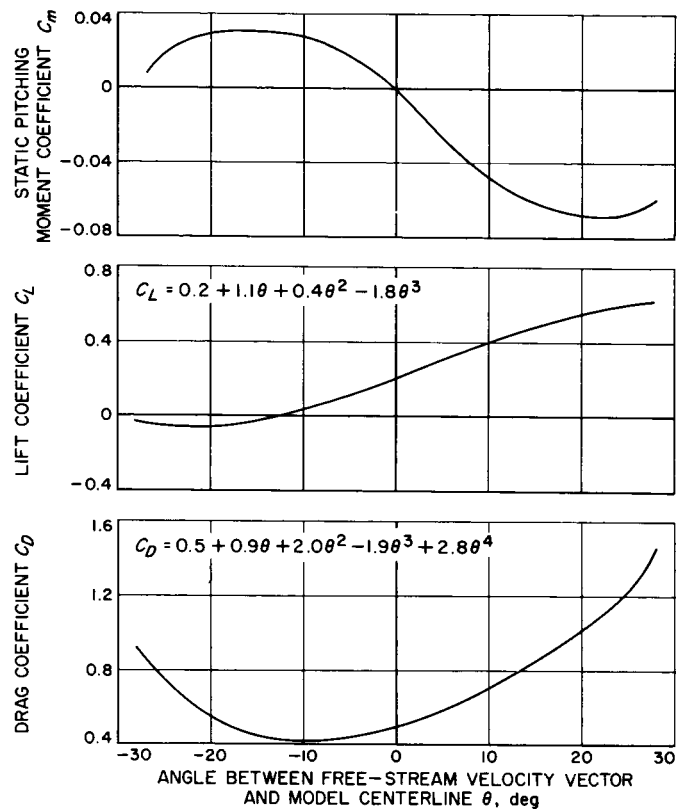
C. Sample Case 2

The static aerodynamics for Sample Case 2 are shown in Fig. 16. As in the first example, an effective constant dynamic stability derivative of -1.0 was used. The static pitching moment is given only in tabulated or plotted form, i.e., without a functional representation. In the previous example, the trajectory characteristics θ'_{max} and $X_{\frac{1}{2}}$ could be generated from the known cubic moment and, therefore, a parametric analysis could be performed prior to experimentation. However, in this case, because an exact functional form for the moment is not available, it is necessary to have measured values of these variables before the determination of the approximating moment

Table 3. Comparison of results using various pitching moment approximations for sample case 1. Input value of $(C_{m_q} + C_{m_{\dot{\alpha}}})$ is -1.0

θ_0, deg	$\delta\theta$, deg	$(C_{m_q} + C_{m_{\dot{\alpha}}})$ (cubic moment)	$(C_{m_q} + C_{m_{\dot{\alpha}}})$ (bi-cubic moment)	$(C_{m_q} + C_{m_{\dot{\alpha}}})$ (bi-linear moment)	$(C_{m_q} + C_{m_{\dot{\alpha}}})$ (offset linear moment)
10.0	0.85	-1.011	-1.076	-0.926	-0.860
15.0	1.25	-1.004	-1.091	-0.871	-0.751
20.0	1.50	-1.002	-1.110	-0.778	-0.624

curves. As determined from the computer-simulated trajectory, $X_{1/2}$ and θ'_{max}, are plotted vs θ_0 in Fig. 17. The positive envelope peaks θ_1, corresponding to particular initial angles $-\theta_0$ were obtained directly from Fig. 16 by using a planimeter, i.e.,

$$\int_{-\theta_0}^{\theta_1} C_m(\theta)\, d\theta = 0$$

The results are shown in Fig. 18. The amplitude decay history, determined from the computer calculations and Fig. 18, is shown in Fig. 19. Finally, the lift and drag terms,

calculated according to Eqs. (46), (47), and (48), are plotted in Fig. 20. The group of Figs. 17–20 comprise the information necessary for the determination of the approximating moment curves and the calculation of the dynamic stability derivative.

The solutions corresponding to the two linear approximating moments are written in terms of the trajectory variables and may be applied directly. The results are listed in Table 4. The offset linear moment does not produce acceptable results; however, the bi-linear moment
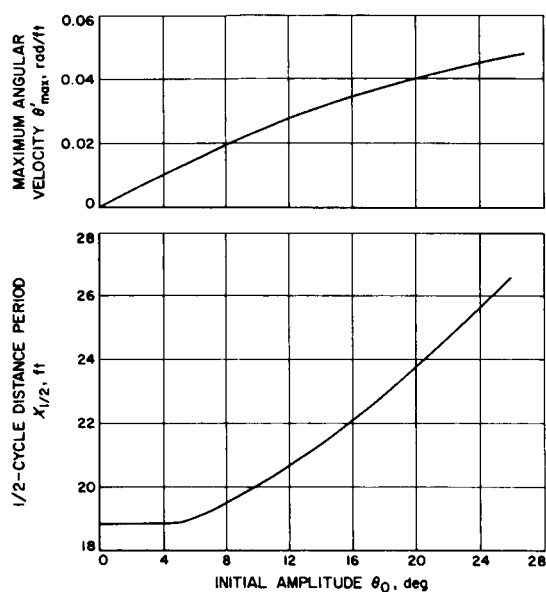

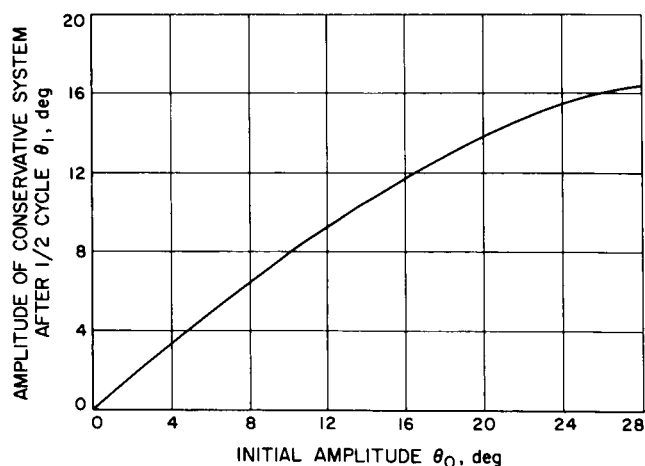Fig. 17. Trajectory characteristics for sample case 2

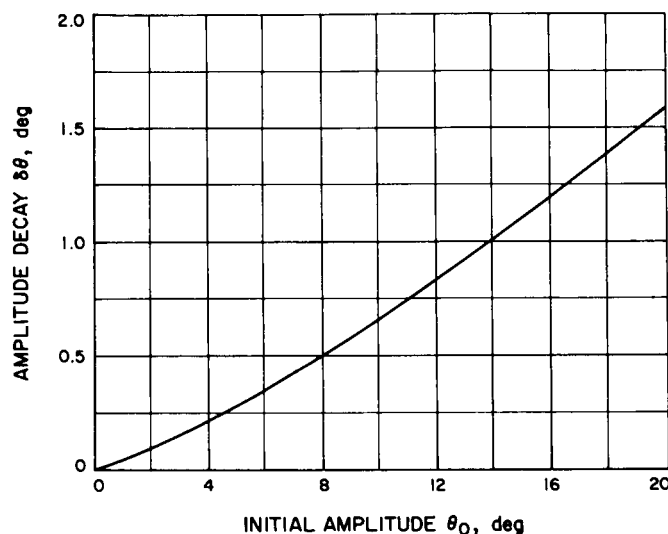Fig. 19. Amplitude decay history for sample case 2

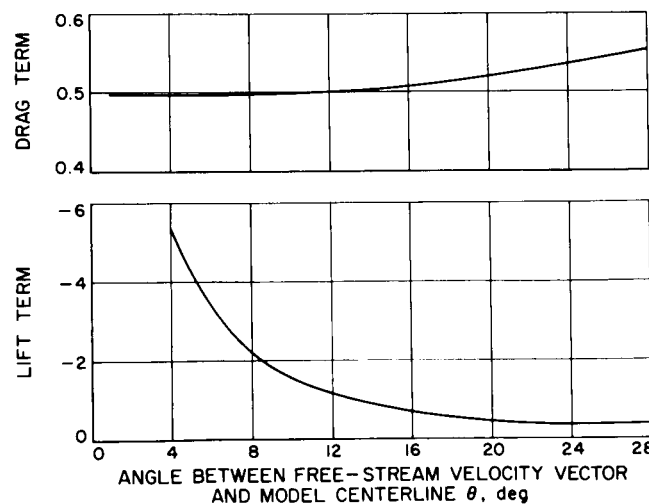Fig. 18. Negative vs positive peaks for sample case 2

Fig. 20. Lift and drag terms for sample case 2

Table 4. Comparison of results using various pitching moment approximations for sample case 2. Input value of $(C_{m_q} + C_{m_{\dot{\alpha}}})$ is -1.0

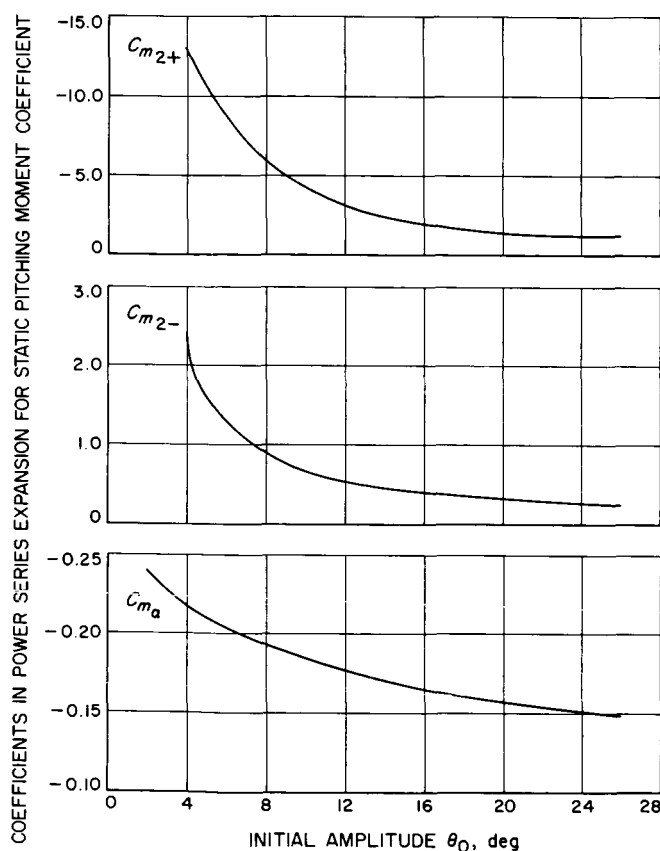| θ_0, deg	$\delta\theta$, deg	$(C_{m_q} + C_{m_{\dot{\alpha}}})$ (cubic moment)	$(C_{m_q} + C_{m_{\dot{\alpha}}})$ (bi-cubic moment)	$(C_{m_q} + C_{m_{\dot{\alpha}}})$ (bi-linear moment)	$(C_{m_q} + C_{m_{\dot{\alpha}}})$ (offset linear moment)
5.0	0.28	-1.018	-1.024	-0.881	-0.816
10.0	0.67	-1.027	-1.039	-0.948	-0.845
15.0	1.13	-1.040	-1.056	-1.029	-0.880
20.0	1.60	-1.046	-1.075	-1.056	-0.867

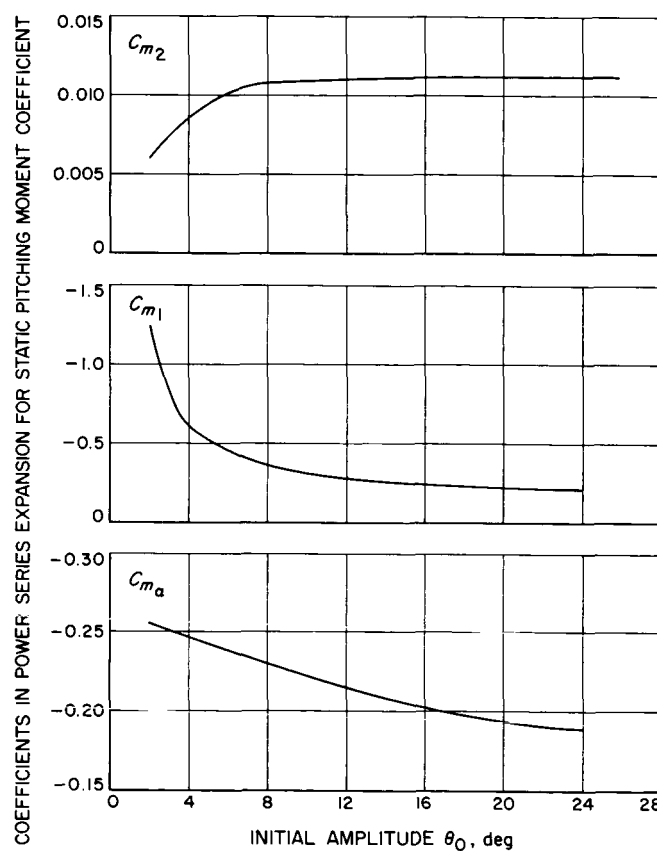**Fig. 21. Equivalent bi-cubic pitching moment, sample case 2**

Fig. 22. Equivalent cubic pitching moment, sample case 2

appears to constitute a very adequate approximation for analysis purposes.

By applying the iterative procedures described in Sections III-C and III-D the two equivalent cubic moments were determined. These approximating curves are shown in Figs. 21 and 22. Equations (62) and (72) were used to calculate $(C_{m_q} + C_{m_{\dot{\alpha}}})$. The results are listed in Table 4. The agreement with the input value of the damping coefficient is quite good for both these moments, the maximum deviation being less than 8%.

V. Summary and Conclusions

Over short time periods, dynamic stability derivatives generally have a relatively small influence on the free-flight angular motion of a vehicle. Observable effects consist of a slight convergence or divergence of the oscillation envelope. The deduction of a damping coefficient from a free-flight trajectory, therefore, requires a very accurate solution to the equation of angular motion. Employing assumptions characteristic to a wind-tunnel application, a solution for the dynamic damping coefficient, in terms

of integrals of the static aerodynamics and trajectory parameters corresponding to a nonaxisymmetric vehicle, was derived in this report. The format of the solution is such that the several quantities contributing to the vehicle amplitude change are completely uncoupled. Therefore, in the final evaluation of the integrals, approximations compatible with the relative importance of each of these parameters may be employed in a term-wise fashion, thereby simplifying the solution without appreciable accuracy loss. In this manner, it was shown that the static pitching moment is the only aerodynamic coefficient involved in the primary term and, as such, constitutes the major limitation on nonlinearity of static aerodynamics. A systematic approach was applied to obtain closed-form solutions corresponding to several functional forms for the static pitching moment, each of increasing complexity and nonlinearity. The last pitching moment considered represents an upper bound with respect to functional generality of the moment representation and practicality of obtaining and applying a solution. In addition, a method of determining an equivalent (for the purpose of analysis) moment curve conforming to any of the considered representations, given the free-flight trajectory and the vehicle's actual pitching moment (in either functional or tabulated form) was discussed. With this device, the equations derived herein may be applied to a body with completely arbitrary static aerodynamics.

The examples demonstrate the validity of the results, as well as the computational procedure. The first example considers a pitching moment conforming exactly to a representation for which a closed-form solution is available. In such a case, a complete analysis can be performed parametrically prior to actual experimentation. Furthermore, the most difficult portion of the computations, the determination of equivalent moment curves, is not required. Calculations of dynamic stability derivatives from a simulated trajectory show excellent agreement with the input values, thereby verifying assumptions made in the development and solution of the equations. The second example considers a static pitching moment given only in tabulated form. In this instance, an *a priori* parametric analysis is not possible because trajectory information is necessary to determine an approximating moment curve. The choice of which functional moment form to use involves a trade-off. The two linear-type approximations require only very simple calculations, but do not lead to as good accuracy as do the nonlinear moments. On the other hand, the nonlinear moments involve iterations and a digital computer for the computations. In some instances, this can lead to a great deal of time and effort in programming and applying an iterative scheme. All four approximating moments were determined and used to provide a comparison of computational accuracies. In this particular example, the bi-linear approximation provides adequate results with a great deal less effort than required by the nonlinear moments and, therefore, is the logical selection for analysis.

In a real application, it might be difficult to anticipate the accuracies of the various approximations solely from an inspection of the true static moment. A good procedure to follow would be to use a simulated trajectory to determine the simplest approximating moment that could be used and still maintain the accuracy requirements. In any instance, it is expected that at least one of the moment forms and corresponding solutions will yield results accurate to within 10%.

Appendix

Iterative Formulas for the Solution of $f(X) = 0$

1. Method of false position.

$$X_{i+1} = \frac{X_i \cdot f(0)}{f(0) - f(X_i)}$$

2. Newton-Raphson method.

$$X_{i+1} = X_i - \frac{f(X_i)}{f'(X_i)}$$

3. Newton's abbreviated method.

$$X_{i+1} = X_i \frac{f(X_i)}{f'(0)}$$

4. Method of accelerated iteration. To apply this method, it must be possible to rewrite the equation in the form $f(X) = g(X) - X = 0$.

Let

$$X_{1_i} = g(X_i), X_{2_i} = g(X_{1_i})$$

Then,

$$X_{i+1} = \frac{X_i X_{2_i} - (X_{1_i})^2}{X_i + X_{2_i} - 2X_{1_i}}$$

Nomenclature

A model reference area, $\pi d^2/4$

$\tilde{a}^2$ elliptic integral parameter

C_A axial force coefficient, axial force/$q_\infty A$

C_D drag coefficient, drag force/$q_\infty A$; C_{D_0}, C_{D_1}, C_{D_2}, C_{D_3}, C_{D_4} are coefficients in power series expansion for drag coefficient

C_L lift coefficient, lift force/$q_\infty A$; C_{L_0}, C_{L_α}, C_{L_1}, C_{L_2} are coefficients in power series expansion for lift coefficient.

C_m static pitching moment coefficient, pitching moment/$q_\infty A d$; C_{m_0}, C_{m_α}, C_{m_1}, C_{m_2} are coefficients in power series expansion for static pitching moment coefficient.

$(C_{m_q} + C_{m_{\dot\alpha}})$ dynamic stability coefficient;

$$\partial Cm/\partial \left(\frac{\dot\theta d}{V}\right) + \partial Cm/\partial \left(\frac{\dot\alpha d}{V}\right)$$

C_N normal force coefficient, normal force/$q_\infty A$

d model diameter, reference length

D drag force

e_z center of pressure offset from reference axis

$E(k, \phi)$ elliptic integral of the second type

$F(k, \phi)$ elliptic integral of the first type

F_A axial force

F_N normal force

g acceleration due to gravity

I model moment of inertia about a transverse axis at center of gravity

$k_\pm$ modulus of elliptic integrals; $\bar{k}_\pm$ is equal to complementary modulus, $\bar{k}^2 = 1 - k^2$

Nomenclature (contd)

k_m $\rho A d / 2I$

l_{cg} distance from model nose to center of gravity

l_{cp} distance from model nose to center of pressure

L lift force

m model mass

M_{cg} sum of moments about the center of gravity

q_∞ free stream dynamic pressure

t time

V model velocity relative to media

V_∞ free stream velocity

x_m model position relative to inertial system along tunnel centerline

X model position relative to media along tunnel centerline

Z, z_m model position in vertical direction

α model angle-of-attack

$\delta\theta$ amplitude decay

θ angle between free-stream velocity vector and model centerline

θ_0 initial amplitude

θ_1 amplitude of conservative system after ½ cycle

μ θ_1/θ_0

$\Pi(k, \tilde{a}^2, \phi)$ elliptic integral of the third type

ρ gas density

ϕ amplitude of elliptic integrals

$(\cdot)$ derivative with respect to time

$(')$ derivative with respect to distance

References

1. Dayman, B., Jr., *Free-Flight Testing in High-Speed Wind Tunnels*, AGARDO-graph No. 113, North Atlantic Treaty Organization, Paris, May 1966.

2. Prislin, R. H., *Free-Flight and Free-Oscillation Techniques for Wind-Tunnel Dynamic-Stability Testing*, Technical Report 32-878, Jet Propulsion Laboratory, Pasadena, Calif., Mar. 1, 1966.

3. Jaffe, P., *Obtaining Free-Flight Dynamic Damping of an Axially Symmetric Body (at All Angles-of-Attack) in a Conventional Wind Tunnel*, Technical Report 32-544, Jet Propulsion Laboratory, Pasadena, Calif., Jan. 15, 1964.

4. Jaffe, P., *A Generalized Approach to Dynamic-Stability Flight Analysis*, Technical Report 32-757, Jet Propulsion Laboratory, Pasadena, Calif., July 1, 1965.

5. Redd, B., Olsen, D. M., and Barton, R. L., *Relationship Between the Aerodynamic Damping Derivatives Measured as a Function of Instantaneous Angular Displacement and the Aerodynamic Damping Derivatives Measured as a Function of Oscillation Amplitude*, NASA TN D-2855, National Aeronautics and Space Administration, Washington, June 1965.

References (contd)

6. Minorsky, N., *Nonlinear Oscillations*, D. Van Nostrand Co., Inc., Princeton, N.J., 1962.

7. Zech, T., *Zum Abklingen nichtlinearer Schwingungen*, Ingenieur-Archiv. XIII, Band, Germany, 1942 (in German).

8. Byrd, P. F., and Friedman, M. D., *Handbook of Elliptic Integrals for Engineers and Physicists*, Springer-Verlag, Berlin, 1954.

9. Uspensky, J. V., *Theory of Equations*, McGraw-Hill Book Co., Inc., New York, 1948.

10. McCracken, D. D., and Dorn, W. S., *Numerical Methods and Fortran Programming*, John Wiley and Sons, Inc., New York, 1964.